ISTANBUL TECHNICAL UNIVERSITY ★ INSTITUTE OF SCIENCE AND TECHNOLOGY

VIBRATION ANALYSIS AND SYSTEM CONTROL OF AERONAUTICAL STRUCTURES

M.Sc. Thesis by
Tuğrul OKTAY

Department : **Aeronautical and Astronautical Engineering**

Programme : **Aeronautical and Astronautical Engineering**

JANUARY 2009

ISTANBUL TECHNICAL UNIVERSITY ★ INSTITUTE OF SCIENCE AND TECHNOLOGY

VIBRATION ANALYSIS AND SYSTEM CONTROL OF AERONAUTICAL STRUCTURES

M.Sc. Thesis by
Tuğrul OKTAY
(511071133)

Date of submission : **25 December 2008**
Date of defence examination: **21 January 2009**

Supervisor (Chairman) : **Prof. Dr. Metin Orhan KAYA (ITU)**
Members of the Examining Committee : **Prof. Dr. İbrahim ÖZKOL (ITU)**
Assoc. Prof. Dr. Erol UZAL (IU)

FEBRUARY 2009

İSTANBUL TEKNİK ÜNİVERSİTESİ ★ FEN BİLİMLERİ ENSTİTÜSÜ

HAVA YAPILARININ TİTREŞİM ANALİZİ VE SİSTEM KONTROLÜ

YÜKSEK LİSANS TEZİ
Tuğrul OKTAY
(511071133)

Tezin Enstitüye Verildiği Tarih : 25 Aralık 2008
Tezin Savunulduğu Tarih : 21 Ocak 2008

Tez Danışmanı : Prof. Dr. Metin Orhan KAYA (İTÜ)
Diğer Jüri Üyeleri : Prof. Dr. İbrahim ÖZKOL (İTÜ)
Doç. Dr. Erol UZAL (İÜ)

ŞUBAT 2009

FOREWORD

I would like to express my gratitude to Prof. Dr. Metin O. Kaya fot his support during my B.Sc. and M.Sc. studies. Also, I would like to express my thanks to my family for their great support.

February 2008 **Tuğrul Oktay**

TABLE OF CONTENTS

Page

LIST OF TABLES ..... **v**
LIST OF FIGURES ..... **vi**
LIST OF SYMBOLS ..... **vii**
SUMMARY ..... **x**
ÖZET ..... **xi**
1. INTRODUCTION **1**
2. CONTROL SYSTEMS **3**
2.1 Control System and its Development 3
2.2 Examples of Control System Applications 4
2.2.1 Smart transportation systems 4
2.2.2 Intelligent systems 4
2.3 Basic Components of a Control Systems 5
2.3.1 Open-loop control systems (Nonfeedback systems) 5
2.3.2 Closed-loop control systems (Feedback control systems) 6
2.4 Transfer Function 6
2.4.1 Single-input, Single-output systems 6
2.4.2 Charactersitic equation 7
2.4.3 Multivariable systems 7
2.5 Block Diagrams 7
2.6 Routh-Hurwitz Criterion 8
2.7 Transient Response of a Prototype Second-Order System 10
2.7.1 Damping ratio and damping factor 11
2.7.2 Natural undamped frequency 12
2.8 Design of Control Systems 15
2.8.1 Design specification 15
2.8.2 Controller configurations 15
2.8.3 Fundamental principle of design 17
2.9 Design with the PD Controller 17
2.10 Control of a Robot Arm 19
2.10.1 Transfer function of a single-joint robot arm 20
2.10.2 Positional controller for a single-joint robot arm 23
3. BEAM FORMULATIONS **26**
3.1 Assumptions for Euler-Bernoulli Beam Theory 26
3.2 Bending Motion of Non-rotating Uniform Euler-Bernoulli Beam 27
3.3 Bending Motion of Rotating Uniform Euler-Bernoulli Beam 28
3.4 Centrifugal Force 29
4. DIFFERENTIAL TRANSFORM METHOD **32**
4.1 History 32
4.2 Definition of Method 32
4.3 Application of Method 33

5. VIBRATION ANALYSIS OF ROTATING TAPERED BEAMS.....35
5.1 Beam Model..... 35
5.2 Equation of Motion and Boundary Conditions..... 36
5.3 Tapered Beam Formulations and Nondimensional Parameters..... 37
5.4 Application of Differential Transform Method..... 38
6. VIBRATION CONTROL OF ROTATING STRUCTURES.....40
6.1 Governing Equations of Rotating Euler-Bernoulli Beam..... 40
6.2 Structural Parameters For Rotating Euler-Bernoulli Beam..... 43
6.3 Block Diagram of Model and Transfer Functions..... 45
6.4 Simulation Results and Discussion..... 47
7. CONCLUSION.....51
REFERENCES.....52
APPENDIX.....53
CURRICULUM VITAE.....55

LIST OF TABLES

Page

Table 2.1: Routh-Hurwitz design..... 9
Table 2.2: Boundary values of damping 15
Table 4.1: Differential transformations of boundary conditions 34
Table 6.1: Effect of taper ratio on beam parameters.....47
Table 6.2: Effect of taper ratio on beam responses.....49
Table 6.3: Effect of taper ratio on the system poles 50

LIST OF FIGURES

Page

Figure 2.1 : Basic components of a control system. 5
Figure 2.2 : Elements of an open-loop control system. 5
Figure 2.3 : Block diagram of a closed-loop control system 6
Figure 2.4 : Subtraction. 8
Figure 2.5 : Addition. 8
Figure 2.6 : Addition and subtraction. 8
Figure 2.7 : Multiplication. 8
Figure 2.8 : Stable and unstable regions in the s-plane. 9
Figure 2.9 : Prototype second-order control system. 10
Figure 2.10 : Unit-Step response of prototype second order system with various damping ratios 11
Figure 2.11 : Relation between characteristic-equation roots of prototype second-damping ratios 13
Figure 2.12 : Constant-Natural-Undamped-Frequency Loci 13
Figure 2.13 : Constant-damping ratio loci. 14
Figure 2.14 : Controlled process 15
Figure 2.15 : Series or cascade compensation 16
Figure 2.16 : Feedback compensation. 16
Figure 2.17 : State-feedback control. 16
Figure 2.18 : Series-feedback compensation. 17
Figure 2.19 : Control system with PD controller 19
Figure 2.20 : Equivalent circuit of an armature-controlled dc motor. 20
Figure 2.21 : Open-loop transfer function of a single-joint robot arm. 23
Figure 2.22 : Feedback control of a single-joint manipulator. 25
Figure 3.1 : Out of plane bending and rotation angle due to bending for Euler Bernoulli beam element. 26
Figure 3.2 : Forces and moments acting on a non-rotating Euler-Bernoulli Beam Bernoulli beam element. 27
Figure 3.3 : Forces and moments acting on a rotating Euler-Bernoulli Beam. 28
Figure 3.4 : Rotating, uniform, clamped-free beam model. 30
Figure 3.5 : Forces and moments acting on a rotating beam element. 30
Figure 5.1 : Double tapered Euler-Bernoulli beam. 36
Figure 6.1 : Euler-Bernaulli Beam with End Mass Attached to a Rigid Hub. 40
Figure 6.2 : Block Diagram of Servomotor Control with Shear Strain Feedback.. 45
Figure 6.3 : Step responses for different taper ratios. 48

LIST OF SYMBOLS

Symbols	Definitions
A	:cross-sectional area (m^2)
c_b	:breath taper ratio
c_h	:height taper ratio
d_b	:path by beam gear (m)
d_m	:path by motor gear (m)
E	:modulus of elasticity (N/m^2)
e	:error function
e_b	:back electomotive force (V)
F	:work done by axial centrifugal force (N.m)
$F(s)$	:characteristic equation
f_b	:viscous-friction coefficient of beam shaft (N.m.s/rad)
f_m	:viscous-friction coefficient of motor shaft (N.m.s/rad)
f_{eff}	:effective viscous-friction coefficient (N.m.s/rad)
$G(s)$	:transfer function
$G_c(s)$	:controller transfer function
$G_H(s)$	:parallel controller transfer function
$G_P(s)$	:controlled process transfer function
I	:area moment of beam cross-section inertia (m^4)
I_b	:area moment of undeformed beam inertia ($kg.m^2$)
I_m	:area moment of motor hub inertia ($kg.m^2$)
i_a	:armature current (A)
i_f	:field current (A)
J_b	:mass moment of beam inertia ($kg.m^2$)
J_m	:mass moment of motor inertia ($kg.m^2$)
K	:gain
$\mathbf{K}$	:shear strain feedback gain
K	:motor gain constant
K_b	:proportionality constant (V.s/rad)
K_D	:derivative gain
K_d	:error derivative feedback gain (V.s/rad)
K_P	:proportional gain
K_p	:position feedback gain (V/rad)

K_T	:motor-torque proportional constant (N.m/A)
L	:laplace transform
L_a	:armature inductance (henry)
L_f	:field inductance (henry)
ℓ	:lenght of beam (m)
M	:bending moment (N.m)
m	:mass per unit lenght (kg/m)
m	:tip mass (kg)
N_b	:number of teeth of beam gear
N_m	:number of teeth of motor gear
n	:gear ratio
PD	:proportional plus derivative
p	:distrubuted load (N/m)
q_i	:ith generalized coordinate
R_a	:armature resistance (ohm)
R_f	:field resistance (ohm)
r	:referance
r_b	:radii of beam gear (m)
r_m	:radii of motor gear (m)
T	:kinetic energy (N.m)
T_m	:motor time constant
t	:time variable (s)
u	:actuating signal
V	:shear force (N)
V	:potential energy (N.m)
V_f	:field voltage (V)
v_P	:inertial velocity of point P (m/s)
v_Q	:tip mass velocity (m/s)
W	:work (N.m)
w	:bending deflection (m)
ω	:frequency
ω	:conditional frequency
ω_i	:ith natural frequency of beam
ω	:natural frequency of control system
y	:controlled varible
α	:damping factor
ϕ	:mode shape
φ_i	:mode participation factor
γ_i	:ratio between dampings
δ	:rotor shaft parameter
η	:rotation speed parameter
η_i	:parameter of natural frequency
θ	:angular displacement of beam shaft (rad)
θ_d	:desired angular displacement of beam shaft (rad)

θ_m	:angular displacement of motor shaft (rad)
ρ	:material density (kg/ m^3)
ρ_i	:frequency ratio
τ	:torque from motor shaft (N.m)
τ_b	:torque on motor (N.m)
τ_m	:torque on beam by referred motor shaft (N.m)
ζ	:damping ratio
Ω	:rotation speed

VIBRATION ANALYSIS AND SYSTEM CONTROL OF AERONAUTICAL STRUCTURES

SUMMARY

In this study, vibration analysis and system control of aeronautical structures has been examined. Firstly, control system has been defined and the steps used for modelling a control system have been introduced. In addition to this, some extra informations to develop controlling model used in this study have been given and transfer functions for general servomotor model have been derived. Afterwards, assumpions for Euler-Bernoulli beam theory have been mentioned and equation of motions for both non-rotating and rotating clamped-free beams with beam theory of Euler-Bernoulli have been found. For derivation of formulations Newton approach has been used. The rules of differential transform method also have been mentioned detailly and listed in a table. Moreover, free vibration analysis of rotating, clamped-free tapered Euler-Bernoulli beam has been done by using differential transform method. And finally, by using dynamic equations and structural parameters which are found by using differential transform method, vibration control of rotating, tapered, clamped-free Euler-Bernoulli beam has been done. When obtained results are compared with the existing results in the literature, it is seen that the designed control system is successful for both positioning of beam and suppression of beam tip vibration. Moreover, it can be easily seen that the increasing height taper ratio has positive effect on beam rotational overshoot. On the other hand, it has lowering effect on amplitude of beam tip vibration.

HAVA YAPILARININ TİTREŞİM ANALİZİ VE SİSTEM KONTROLÜ

ÖZET

Bu çalışmada, dönen hava yapıların titreşim analizi yapılmış ve sistem kontrolü sağlanmıştır. Çalışmada ilk olarak, kontrol sistemi tanımlanmış ve bir kontrol sisteminin modellenmesi için gerekli adımlar anlatılmıştır. Buna ilaveten, bu çalışmada kullanılan kontrol sisteminin oluşturulması için gerekli adımlar anlatılmıştır ve genel doğru akım motor yapısının transfer fonksiyonları elde edilmiştir. Daha sonrasında ise Euler-Bernoulli kiriş teorisi için yapılan genellemeler anlatılmış, dönen ve dönmeyen durumda ankastre bir kirişin hareket denkleminin çıkarılışı Euler-Bernoulli kiriş teorisiyle birlikte bulunmuştur. Bu sırada Newton yaklaşımından yaralanılmıştır ve sonrasında diferansiyel dönüşüm yönteminin kuralları detaylı bir şekilde anlatılmış ve bir tabloda listelenmiştir. Ayrıca, dönen ve daralan ankastre Euler-Bernoulli kirişinin serbest titreşim analizi diferansiyel dönüşüm yöntemiyle gerçekleştirilmiştir. Son olarak dinamik denklemler ve daha önce diferansiyel dönüşüm yöntemi yardımıyla bulunan yapısal parametrelerle dönen ve daralan, ankastre Euler-Bernoulli kirişinin titreşim kontrolü gerçekleştirilmiştir. Bulunan sonuçlar literatürdeki çalışmalarla karşılaştırıldığında, kullanılan kontrol sisteminin kirişin belli bir konuma oturtulmasında ve bu sırada oluşun titreşimleri sönümlemede başarılı olduğu görülebilir. Ayrıca, artan yükseklik daralma oranının kirişin belli bir pozisyona otururken oluşan maksimum aşımda arttırıcı bir etkisinin olduğu ve öte yandan bu sırada kiriş ucunda oluşan titreşim genliğinde azaltıcı bir etkisi olduğu görülebilir.

1. INTRODUCTION

Recently, the problem of modeling and control of a rotating flexible beam has taken great attention with the applications such as rotating flexible beams, model robot arms, elastic linkages, disk drive actuators, turbomachinary blades, helicopter rotors, spinning spacecrafts and like systems. The demands have been increasing the speed of operation and reducing the power consumption which encourages the use of light-weight materials. Also, the research interest in flexible manipulators which is examined in this master thesis such as light-weight and large dimensions robotic manipulators, has incresed significantly in recent years. Major advantages of flexible manipulators include small mass, fast motion and large force to mass ratio for reduced energy consumption, increased productivity and enhanced payload capacity. However, flexible robotic manipulators also impose various challenges in research in comparison to rigid robotic manipulators, ranging from system design, structrural optimization construction to modeling, sensing and control as stated **Wang and Gao (2003)**. For example, current industrial approaches to robot arm control system design behave each joint of the robot arm as a simple joint servomechanism. This servomechanism approach models the varying dynamics of a manipulator inadequately since it ignores the motion and configuration of the whole arm mechanism. These changes in the parameters of the controlled system are significant enough to make conventional feedback control strategies ineffective which causes reduced servo response speed and damping, limited precision and speed of the end-effector and use of it appropriate only for limited-precision tasks as stated **Fu and Gonzales (1987)**. Therefore, manipulators controlled this way can move only at slow speeds with unnecessary vibrations. Any significant performance in this and other areas of robot arm control requires the consideration of more efficient dynamic models, sophisticated control techniques and use of computer architectures.

In the first part of the thesis, control system has been defined and the steps used for modelling a control system have been introduced. In addition to this, some extra informations to develop controlling model used in this study have been given.

Firstly, structure of a control system has been examined. During this examination, basic components of a control system, transfer functions, block diagrams are mentioned. Secondly, Routh-Hurwitz Criterion is defined and transient response of a prototype second-order system is examined. Also, design of a control system is introduced. Finally, transfer function of a single-joint robot arm is derived. Also, by using this position controller for a single joint manipulator is designed.

In the second part of the thesis, equation of motion for both non-rotating and rotating clamped-free beams with beam theory of Euler-Bernoulli have been found. For derivation of formulations Newton approach has been used. Also, by using this free vibration analysis of rotating tapered Euler-Bernoulli beams have been done with DTM.

In the final part of the thesis, by using dynamic equations and structural parameters found with DTM vibration control of tapered, clamped-free Euler-Bernoulli beam has been done. Obtained results are compared with the existing results in the literature, it is seen that the designed control system is successful for both positioning of beam and suppression of beam tip vibration.

2. CONTROL SYSTEM DESIGN

In this chapter control system is defined and the steps used for modelling a control system are introduced. In addition to this, some extra informations to develop controlling model used in this study are given.

2.1 Control System and its Development

To define a control system as stated **Kuo and Golnaraghi (2003)**, it can be mentioned about daily life there are many objectives that need to be achieved . For example, in the domestic domain, it is needed to regulate the temperature and humidity of houses and buildings for comfort. For transportation, it is needed to control the automobile and airplane to go from one place to other on time and safely. Industrially, manufacturing process contain numerous aims for products that will satisfy the precision and cost effectiveness necessities. A human being is capable of performing a wide range of tasks, including decision making. Some of these tasks, such as picking up objects and walking from one point to another, are widely carried out in daily routine. Under certain conditions, some of these tasks are to be performed in the best possible way. The maens of accomplishing these objectives generally require the use of control systems that implement certain control strategies.

Recently, control systems have assumed and increasingly important role in the development and advancement of modern civilization and technology. Pratically every aspect of our day-to-day activities is affected by some type of control systems. Control systems are found in abundance in all sectors of industry, such as quality control of manufacturing products, automatic assemlyline, machine-tool control, space technology and weapon systems, computer control, transportation systems, power systems, robotics, MicroElectroMechanical Systems (MEMS), nanotechnology, and many others. Even the control of inventory and social and economic systems may be approached from the theory of automatic control.

2.2 Examples of Control-System Applications

2.2.1 Smart transportation systems

Perhaps one of the most innovative fields in controls used in consumer products is that of the automative industry. We have grown to desire cars that are intelligent and provide maximum levels of comfort, safety, and fuel efficiency. Examples of intelligent systems in cars include climate control, cruise control, antilock brake systems (ABSs), active suspensions that reduce vehicle vibration over rough terrain, air springs that self-level the vehicle in high-G turns (in addition to providing beter ride), integrated vehicle dynamics that provide yaw control when the vehicle is either over-or understeering (by selectively activating the brakes to regain vehicle control), trancation control systems to prevent spinning of wheels during acceleration, active sway bars to provide 'controlled' rolling of vehicle.

2.2.2 Intelligent systems

Applications of control systems have significantly increased through the development of new materials, which provide unique oppurtunities for highly efficient actuation and sensing, therby reducing energy losses and environmental impacts. State-of-the-art actuators and sensors may be implemented in virtually and system, including biological propulsion; locomotion; robotics, material handling; biomedical, surgical, and endoscopic; aeronautics; marine; and the defense and space industries. Potential applications of control these systems may benefit the following areas as used in **Kuo and Golnaraghi (2003)**:

- Machine tools: Improve precision and increase productivity by controlling chatter.
- Flexible robotics: Enable faster motion with greater accuacy.
- Photolithography: Enable the manufacture of smaller microelectronic circuits controlling vibration in the photolithography circuit-printing process.
- Process control: For example, on/off shape control of solar reflectors or aerodynamic surfaces.

2.3 Basic Components of a Control System

The main parts of a control system can be described by as below:

1. Objectives of control
2. Control-system components
3. Results or outputs

The main realtionship between these three components is shown in Figure 2.1. In more technical terms, the objective can be identified with inputs, or actuating signals, u, and the results are also called outputs, or, controlled variables, y. Genearlly, the main idea of the control system is to control the outputs in some prescribed manner by the inputs with the elements of the control system.



Figure 2.1: Basic components of a control system

2.3.1 Open-Loop Control Systems (Nonfeedback Systems)

The parts of an open-loop control system can be generally divided to two main parts which are controller and the controlled process shown in Figure 2.2. In this block diagram input signal r is applied to the controller, whose output behaves as the actuator signal u , the actuating signal then controls the controlled process so that the controlled variable y perform according to some prescribed manners.

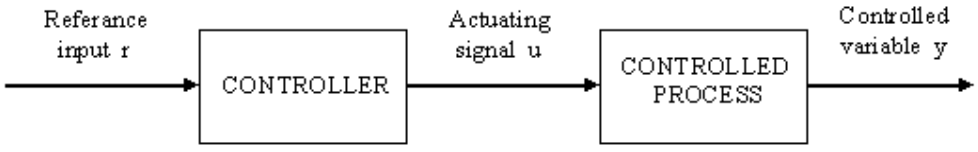


Figure 2.2: Elements of an open-loop control System

2.3.2 Closed-loop control systems (Feedback control systems)

When some or all output signal from a system, perhaps altered in some way, is summed with the original input signal to produce a modified input signal, it is called as feedback control system whose block diagram is shown Figure 2.3.

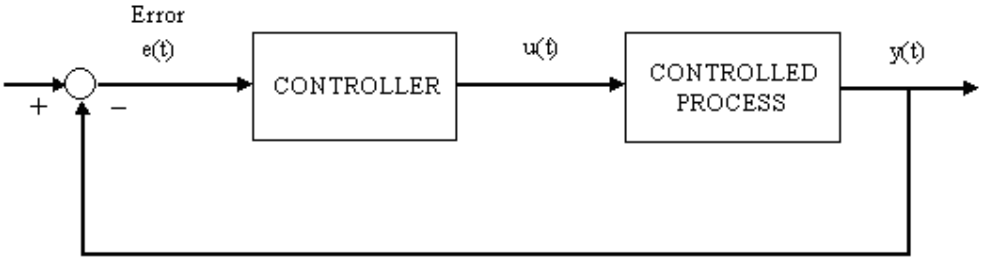


Figure 2.3: Block diagram of a closed-loop control system

2.4 Transfer Function

2.4.1 Single-Input, Single-Output Systems

The transfer function of a linear time –invariant system is defined as the Laplace transform of the impulse response, with all the initial conditions to zero. For example, G(s) is the transfer function of a single-input, single output system with input u(t), output y(t), and impulse response g(t). The transfer function G(s) is defined here as in Equation (2.1).

$$G(s)=L[g(t)]=\frac{Y(s)}{U(s)} \qquad \textbf{(2.1)}$$

Although the transfer function of a linear system is defined in terms of the impulse response, in prctice, the the raltion between the output and input of a linear time-invariant system with continous-data input is generally described by a differential equation so that the transfer function can be written as in Equation (2.2) .

$$G(s)=\frac{Y(s)}{U(s)}=\frac{b_m s^m+b_{m-1}s^{m-1}+.....+b_1 s+b_0}{a_n s^n+a_{n-1}s^{n-1}+.....+a_1 s+a_0} \qquad \textbf{(2.2)}$$

2.4.2 Characteristic equation

The characteristic equation of a linear system is defined the equation obtained by setting the denominator polynomial of the transfer function to zero. Hence, it is as described in Equation (2.3).

$$s^n + a_{n-1}s^{n-1} + ... + a_1 s + a_0 = 0 \quad \textbf{(2.3)}$$

2.4.3 Multivariable Systems

In simple way the definition of transfer funtion can be extended to a system which has multiple input and output. This system is often called as a multivariable system. Because the principle of superposition is valid for linear systems, the total effect on any output due to all the inputs acting simultaneously is obtained by adding up the outputs due to each input acting alone. It is shown in Equations (2.4) and (2.5) as below.

$$G_{ij} = \frac{Y_i(s)}{R_j(s)} \quad \textbf{(2.4)}$$

$$Y_i(s) = G_{i1}R_1(s) + G_{i2}R_2(s) + ... + G_{ip}(s)R_p(s) \quad \textbf{(2.5)}$$

Here, i=1,2,....,q (q is the number of outputs) and j=1,2,....,p (p is the number of inputs).

2.5 Block Diagrams

Since their simplicity and versatility, block diagrams are often used by control designers to model all types of systems.It can be used easily to describe the composition and interconnection of a system. If the mathematical and functional realtionships of all the systems elements are given, the block diagram may be used as a tool for the analytic or computer solution of the system. Their algebra is shown in Figures 2.4 - 2.7 below as defined in **Kuo and Golnaraghi (2003)**.

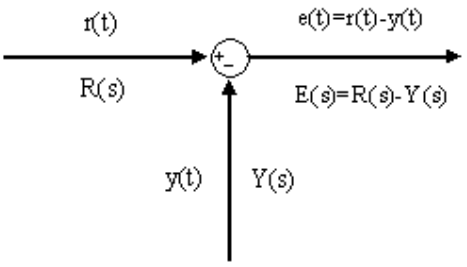


Figure 2.4: Subtraction

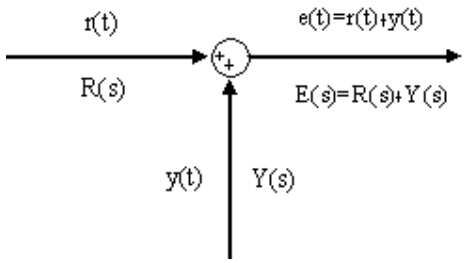


Figure 2.5: Addition

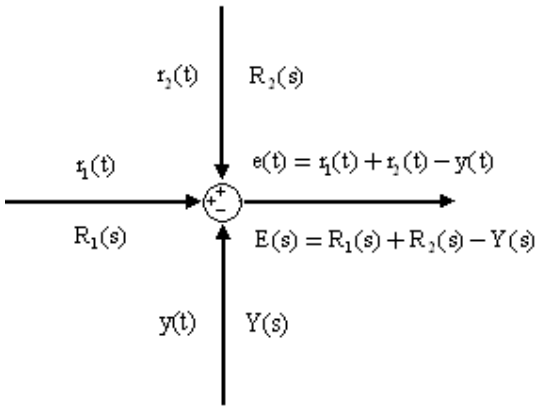


Figure 2.6: Addition and subtraction

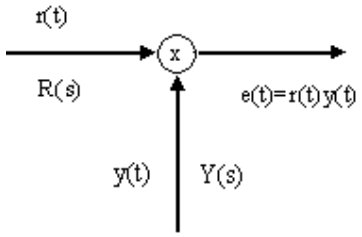


Figure 2.7: Multiplication

2.6 Routh-Hurwitz Criterion

This criterion is an algebraic method that provide information on the absolute stability of a linear time-invariant system that has characteristic equation with constant coefficients. The Routh-Hurwitz criterion represents a method of determining the location of determining the location of zeros a polynomial with constant real coefficients with respect to the left half and right half the s-plane shown in Figure 2.8, without actually solving the zeros. Since root-finding computer program can solve for the zeros of a polynomial with ease, the value of the Routh-Hurwitz criterion is at best limited to equations of a linear time varient SISO system is the form in Equation 2.6 as stated by **Kuo and Golnaraghi (2003)**.

$$F(s) = a_n s^n + a_{n-1} s^{n-1} + ... + a_1 s + a_0 = 0 \qquad \textbf{(2.6)}$$

where all the coefficients are real. In order that the last equation does not have roots

with positive real parts, it is necessary (but not sufficient) that the following conditions hold:

1. All the coefficients of the equation have the same sign.

2. None of the coefficients vanishes.

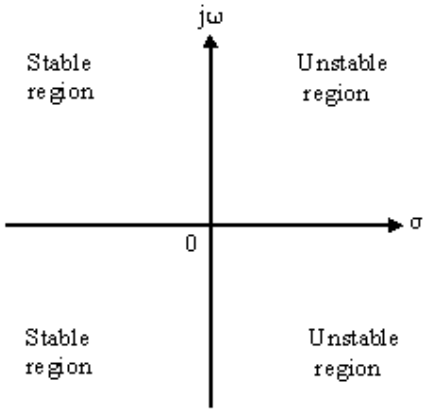


Figure 2.8: Stable and unstable regions in s-plane

A tabular method can be used to determine the stability when the roots of a higher order characteristic polynomial is difficult to obtain. For an n – th order polynomial as Equation (2.6) a table as Table 2.1 having n rows and the following structure can be used.

Table 2.1: Routh-Hurwitz design

a_n	a_{n-2}	a_{n-4}	.....
a_{n-1}	a_{n-3}	a_{n-5}	.....
b_1	b_2	b_3	.....
c_1	c_2	c_3	.....
.....	.....	.....	.....

Here, the elements b_1 and c_1 can be computed as in Equations (2.7) and (2.8).

$$b_1 = \frac{a_{n-1}a_{n-2} - a_n a_{n-3}}{a_{n-1}} \quad \textbf{(2.7)}$$

$$c_1 = \frac{b_1 a_{n-3} - b_2 a_{n-1}}{b_1} \quad \textbf{(2.8)}$$

When completed this table, the number of sign changes in the first column will be the number of non-negative poles.

2.7 Transient Response of a Prototype Second-Order System

Although true second-order control systems are rare in practice, their analysis generally helps to form a basis for understanding of analysis and design of higher-order systems, especially the ones that can be approximated by second-order systems. Considering that a second-order control system with unity feedback is reperesented by the block diagram shown in Figure 2.9. The open-loop transfer function of the system is as in Equation (2.9).

$$G(s)=\frac{Y(s)}{E(s)}=\frac{\omega_n^2}{s(s+2\zeta\omega_n)} \tag{2.9}$$

where ζ and ω_n are real constants.Also, the closed-loop transfer function of the system is as in Equation (2.10).

$$\frac{Y(s)}{R(s)}=\frac{\omega_n^2}{s^2+2\zeta\omega_n s+\omega_n^2} \tag{2.10}$$

The system shown in Figure 2.9 with the transfer function given in Equations (2.9) and (2.10) is defined as the prototype second-order system.

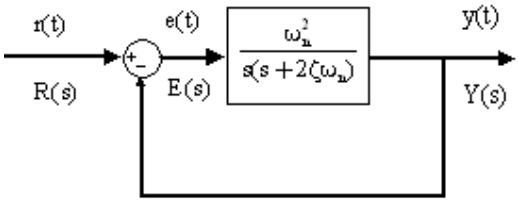


Figure 2.9: Prototype second-order control system

The characteristic equation of the prototype second-order system is obtained by setting the denominator of Equation (2.10) to zero as in Equation (2.11).

$$\Delta(s)=s^2+2\zeta\omega_n s+\omega_n^2=0 \tag{2.11}$$

For a unit-step response input, R(s)=1/s, the output response of the system is obtained by taking the inverse Laplace transform of the output transform as in Equation (2.12).

$$Y(s)=\frac{\omega_n^2}{s(s^2+2\zeta\omega_n s+\omega_n^2)} \tag{2.12}$$

The result is found as below in Equation (2.13).

$$y(t) = 1 - \frac{e^{-\zeta\omega_n t}}{\sqrt{1-\zeta^2}} \sin(\omega_n \sqrt{1-\zeta^2}\, t + \cos^{-1}\zeta, \qquad t \geq 0 \tag{2.13}$$

Figure 2.10 shows the unit-step response of Equation (2.13) plotted as functions of the normalized time $\omega_n t$ for various values of ζ. From that, the response becomes more oscillatory with larger overshoot as ζ decreases. While $\zeta \geq 1$, the step response does not show any overshoot. Thus, y(t) never exceeds its final value during transient.

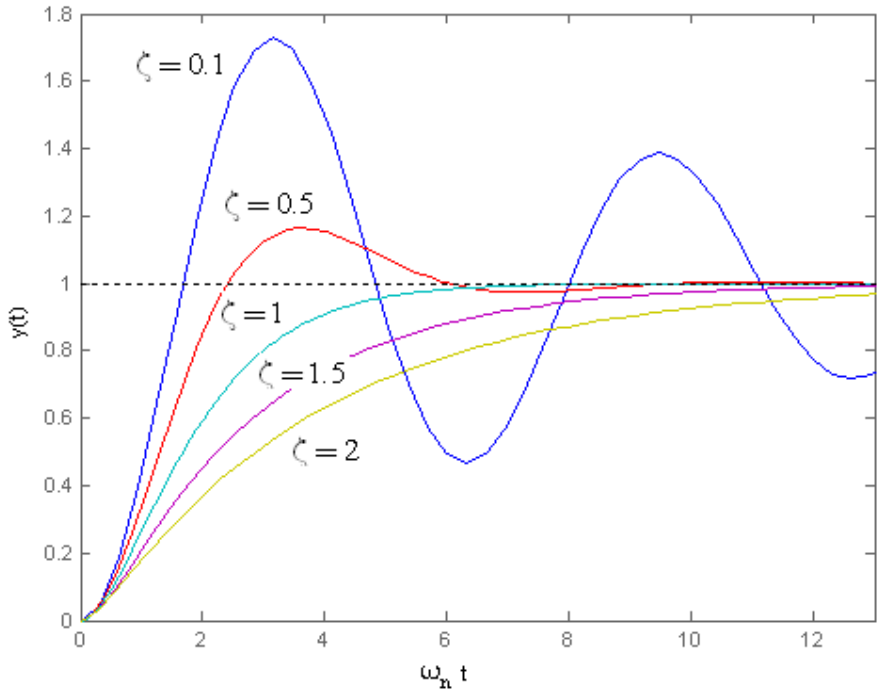


Figure2.10: Unit-Step response of prototype second order system with various damping ratios

2.7.1 Damping ratio and damping factor

The effects of the system parameters ζ and ω_n on the step response y(t) of the prototype second-order system can be examined with the roots of the characteristic equation in Equation (2.11). The two roots can be expressed as in Equation (2.14).

$$s_1, s_2 = -\zeta\omega_n \pm j\omega_n\sqrt{1-\zeta^2} = -\alpha \pm j\omega \tag{2.14}$$

here α and ω are shown in Equations (2.15) and (2.16) as below

$$\alpha = \zeta\omega_n \tag{2.15}$$

$$\omega = \omega_n\sqrt{1-\zeta^2} \tag{2.16}$$

The physical importance of ζ and α is examined here. From Equations (2.13) and (2.15), α is seen as the constant that is multiplied to t in the exponential term of y(t). Hence, α controls the "damping" of the system, and is called the damping factor or damping constant. The inverse of α, $1/\alpha$, is proportional to the time constant of the system. While the two roots of characteristic equation are real and equal, the system is called critically damped. By using Equation (2.14) it can be seen that critical damping occurs when ζ=1. Under this condition, the damping factor is easily $\alpha = \omega_n$. Therefore, it can be regarded ζ as the damping ratio, shown in Equations (2.17) as below and (2.18) used when the roots are at the left-half s-plane.

$$\zeta = \text{damping ratio} = \frac{\alpha}{\omega_n} = \frac{\text{Actual damping factor}}{\text{damping factor at critical damping}} \tag{2.17}$$

2.7.2 Natural undamped frequency

The parameter ω_n is defined as the natural undamped frequency. From the Equation (2.14) when ζ=0, the damping is zero. Also, the roots of the characteristic equation are imaginary, and by using Equation (2.13) the unit-step response is purely sinusodial.Thus, ω_n corresponds to the frequency of the undamped sinusodial response. Using Equation (2.14) when $0<\zeta<1$, the imaginary part of the roots has the magnitude of ω. When $\zeta \neq 0$, the response of y(t) is not a periodic function, and ω defined in equation a is not a frequency. It is defined as the conditional frequency, or the damped frequency .

$$\zeta = \cos\theta \tag{2.18}$$

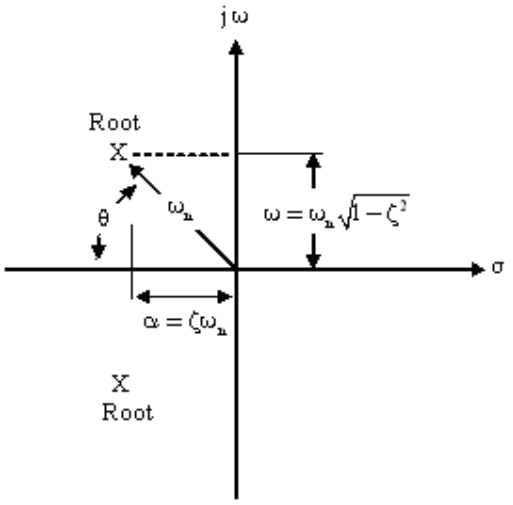


Figure 2.11: Relation between characteristic-equation roots of prototype second-order system and α, ζ, ω_n, and ω.

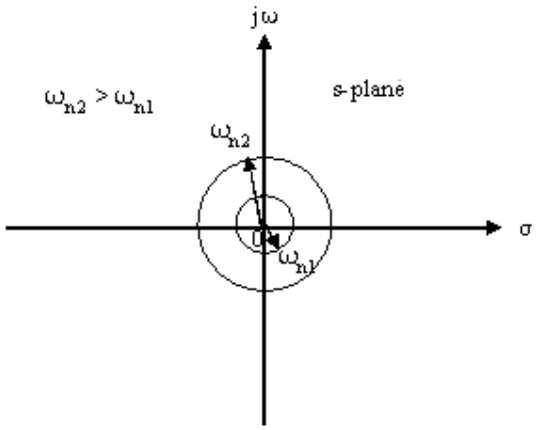


Figure 2.12: Constant-Natural-Undamped-Frequency Loci

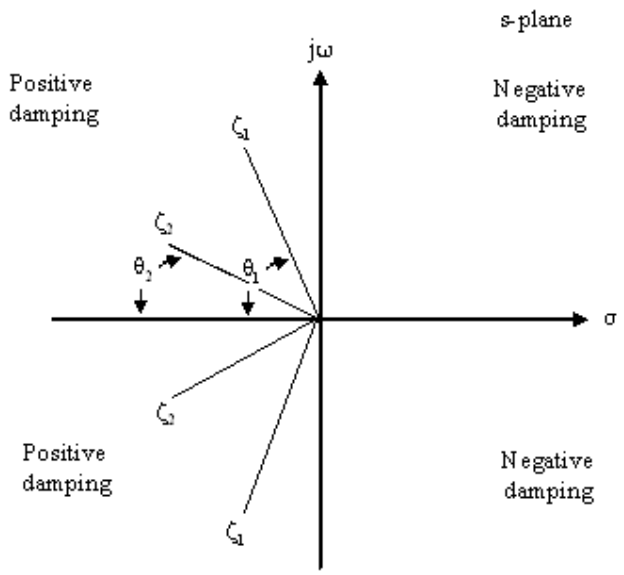


Figure 2.13: Constant-damping ratio loci

The left-half s plane corresponds to positive damping, that is, the damping factor or damping ratio is positive that causes the unit-step response to settle to a constant final value in the steady state due to the negative exponent of $\exp(-\zeta\omega_n t)$. Therefore, the system is stable.

The right-half s-plane coreesponds to negative damping taht gives a response that grows in magnitude without bound with time. Hence, the system is unstable.

The imaginary axis corresponds to zero damping ($\alpha = 0$ or $\zeta = 0$). Zero damping causeses sustained oscillation response, and the system is marginally stable or marginally unstable.

Finally, it can be seen that the location of the characteristic equation roots of the simple prototype second-order system have significant role in the transient response of the system. Since damping is very important to examine dynamic system, its boundary values are shown Table 2.2 below.

Table 2.2 : Boundary Values of Damping

$\zeta < 0$	$s_1, s_2 = -\zeta\omega_n \pm j\omega_n\sqrt{1-\zeta^2}$	negatively damped
$\zeta = 0$	$s_1, s_2 = \pm j\omega_n$	undamped
$0 < \zeta < 1$	$s_1, s_2 = -\zeta\omega_n \pm \omega_n\sqrt{1-\zeta^2}$	underdamped
$\zeta = 1$	$s_1, s_2 = -\omega_n$	critically damped
$\zeta > 1$	$s_1, s_2 = -\zeta\omega_n \pm \omega_n\sqrt{\zeta^2-1}$	overdamped

2.8 Design of Control Systems

2.8.1 Design specifications

Design specifications are generally used to describe what the system should do and how it is done. These are relative stability,steady-state accuracy (error), transient-response, and frequency-response characteristics. In some complex applications there can be some extra specifications such as sensitivity to parameter variations, that is, robustness.

2.8.2 Controller configurations

Generally, the dynamics of linear controlled process can be defined by the block diagram shown below in Figure 2.15.

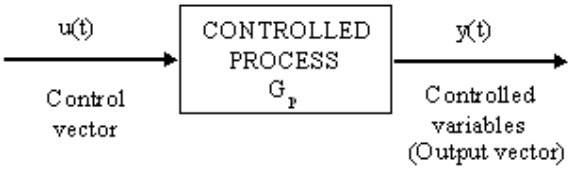


Figure 2.14: Controlled process

The main design objective is controlling the output vector y(t), behave in certain desirable ways. The problem essentially requires the determination of the control signal u(t) over the prescribed time interval so that the design objectives are all satisfied. In most of the widely used design methods designer knows the place where the controller is to be positioned relative to the controlled process. The problem then requires the design of the elements of the controller. Since most control efforts

involve the compensation of the system-performance characterstics, the general design using fixed configuration is also called compensation. Types of compensations are shown in Figs. 2.15- 2.18 below as defined in **Kuo and Golnaraghi (2003)**.

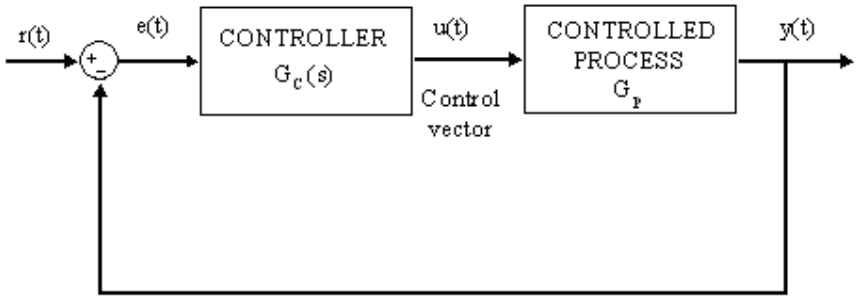


Figure 2.15: Series or cascade compensation

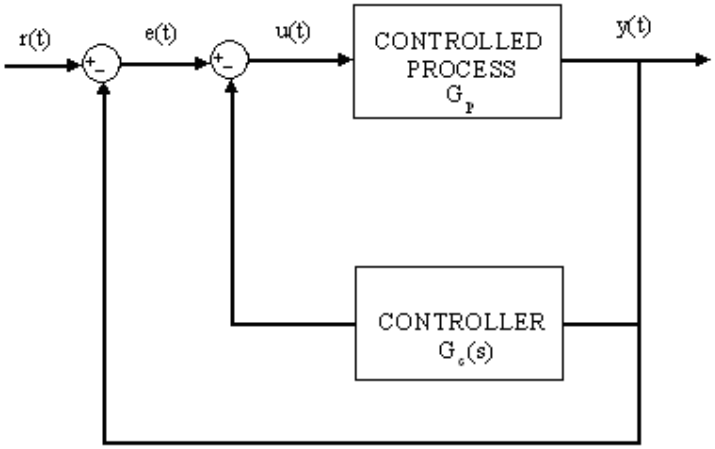


Figure 2.16: Feedback compensation

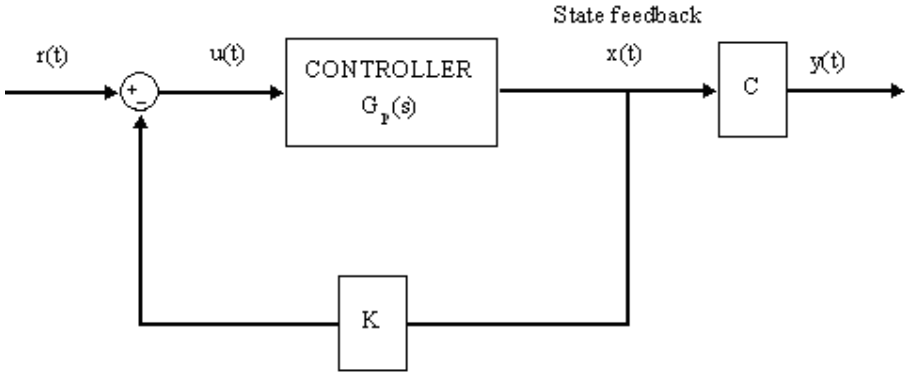


Figure 2.17: State-feedback control

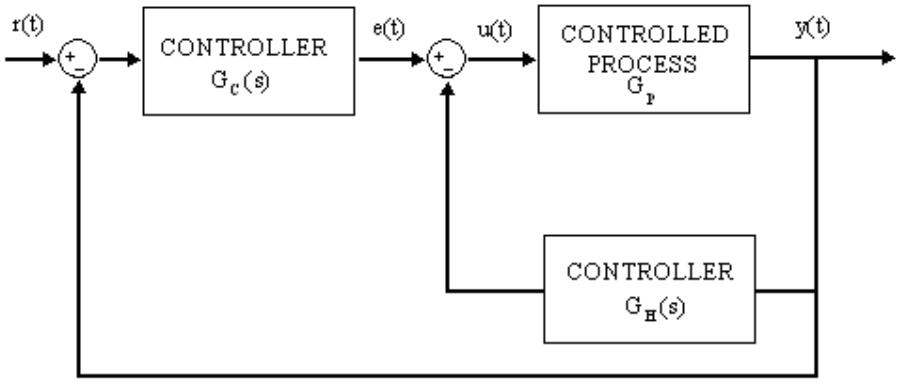


Figure 2.18: Series –feedback Compensation

Figure 2.15 shows the most widely used system configuration with the controller placed in series with the controlled process, and the condiguration is referred to as series or cascade compensation.

In Figure 2.16 the controller is placed in the mirror feedback path, and the scheme is named feedback compensation.

Figure 2.17 shows a system that generates the control signal by feeding back the state variables through constant real gains, and the scheme is called state feedback.

Figure 2.18 shows the series-feedback compensation for which a series controller and feedback controller are used.

2.8.3 Fundamental principle of design

After selecting a controller configuration, the designer must choose a controller type with proper selection of its element values satisfying all the design specifications.After choosing conroller, the next step is to choose controller parameter values that typically the coefficients of one or more transfer functions making up the controller.The basic design approach is using the analysis tools to maintain how individual parameter values influence the design specification, and finally system performance.

2.9 Design with the PD Controller

In simple control systems , the controller is typically a simple amplifier with a constant gain K. This type of control is known as proportional control, because the

control signal at the output of the controller is directly related to the input of the controller by a proportional constant. Intuivitely, it can be used that the derivative or integral of the input signal, in addition to the proportional operation. Therefore, it may be considered that a more general continous-data controller to be one taht contains such components as adders like amplifiers, attenuators, differentiators, and integrators. Determining which of these components should be used is the main task of designer. PD controller is type of these which is examined here. Figure 2.19 as below shows the block diagram of a feedback control system that arbitrarily has a second-order prototype process with the transfer function in Equation (2.19).

$$G_P(s) = \frac{\omega_n^2}{s(s + 2\zeta\omega_n)} \tag{2.19}$$

The series controller is a proportional-derivative (PD) type with the transfer function by Equation (2.20) as below.

$$G_c(s) = K_P + K_D s \tag{2.20}$$

Hence, the controller signal applied to the process is found as in Equation (2.21).

$$u(t) = K_P e(t) + K_D \frac{de(t)}{dt} \tag{2.21}$$

where s is as Equation (2.22).

$$s = -\frac{K_P}{K_D} \tag{2.22}$$

where K_P and K_D are the proportional and derivative constants, respectively. The forward-path transfer function of the compensted system is shown in Equation (2.23).

$$G(s) = \frac{Y(s)}{E(s)} = G_c(s)G_p(s) = \frac{\omega_n^2(K_P + K_D s)}{s(s + 2\zeta\omega_n)} \tag{2.23}$$

which shows that the PD control is equivalent to adding a simple zero at $s = -\frac{K_P}{K_D}$ to the forward-path transfer function.

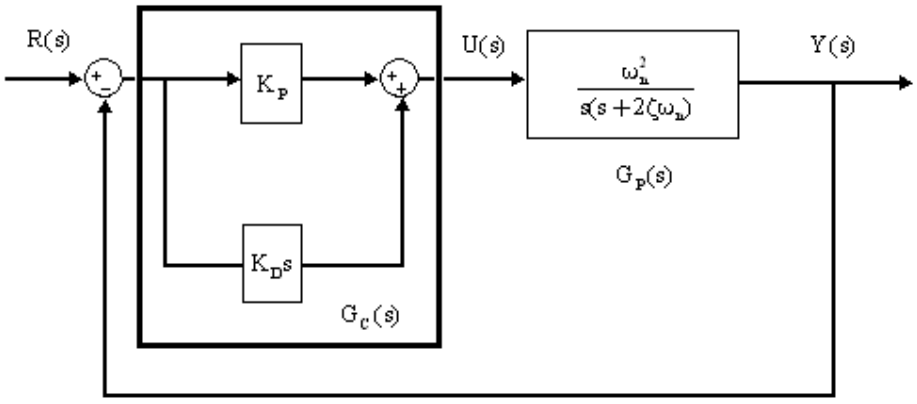


Figure 2.19 : Control system with PD controller

Also, summary of effects of PD control can be written. Although it is not effective with lightly damped or initially unstable systems, a properly design PD controller can affect the performance of a control system as below:

1. Improving damping and reducing maximum overshoot.
2. Reducing rise time and settling time.
3. Possibly accentuating noise at higher frequincies

2.10 Control of a Robot Arm

Most industrial robots are either electrically, hydraullically, or pneumatically actuated. Electrically driven manipulators are constructed with a dc permanent magnet torque motor for joint. Mainly, the dc torque motor is apermanent magnet, armature excited, continous rotation motor with some features that high torque-power ratios, smooth, low-speed operation, linear torque-speed characteristics, and short time constants. In Figure 2.20 an equivalent circuit of an armature-controlled dc magnet torque motor for a joint is shown as in **Fu and Gonzales (1987)**.

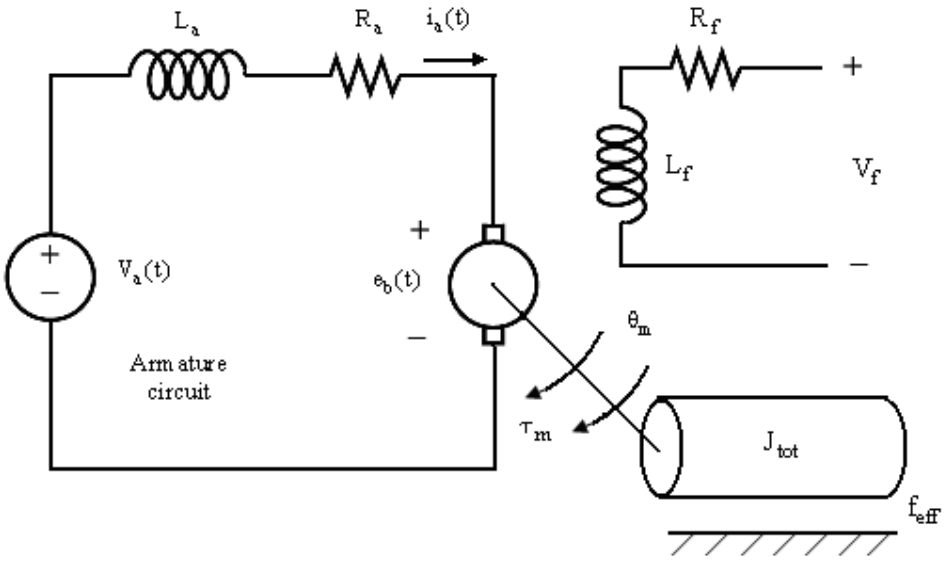


Figure 2.20: Equivalent circuit of an armature-controlled dc motor

Here i_a is the armature current, i_f is the field current, e_b is the back electomotive force, V_a is the armature voltage, V_f is the field voltage, L_a is the armature inductance, L_f is the field inductance, R_a is the armature resistance and R_f is the field resistance.

2.10.1 Transfer function of a single joint robot arm

This part deals with the derivation of the transfer function of a single joint robot arm from which a proportional plus derivative controller (PD controller) is getted. Firstly, the radius and angle-radii relation between motor and beam is written as in Equation (2.24).

$$d_m = d_b \quad \text{and} \quad r_m\theta_m = r_b\theta \tag{2.24}$$

Since the radius of the gear is proportional is proportional to number of teeth, the Equation (2.25) can be written as below.

$$N_m\theta_m = N_b\theta \quad \text{and} \quad \frac{N_m}{N_b} = \frac{\theta}{\theta_m} = n < 1 \tag{2.25}$$

Here n is the gear ratio and the relations between angles may be used as in Equation (2.26).

$$\theta(t) = n\theta_m(t) \tag{2.26}$$

By taking the first two derivatives of them it can be obtained as in Equation (2.27).

$$\dot{\theta}(t) = n\dot{\theta}_m(t) \quad \text{and} \quad \ddot{\theta}(t) = n\ddot{\theta}_m(t) \tag{2.27}$$

If a load is attached to beam gear, then the torque developed at the motor shaft is equal to sum of the torques dissipated by the motor and its load as in Equation (2.28) as stated **Fu and Gonzales (1987)**.

$$\begin{pmatrix}\text{Torque from}\\ \text{motor}\\ \text{shaft}\end{pmatrix} = \begin{pmatrix}\text{Torque}\\ \text{on}\\ \text{motor}\end{pmatrix} + \begin{pmatrix}\text{Torque on load}\\ \text{referred to}\\ \text{the motor shaft}\end{pmatrix}$$

$$\tau(t) = \tau_m(t) + \tau_b^*(t) \tag{2.28}$$

In addition to this, the load torque related to the load shaft and the motor torque related to the motor shaft are as in Equations (2.29) and (2.30).

$$\tau_b(t) = J_b\ddot{\theta}(t) + f_b\dot{\theta}(t) \tag{2.29}$$

$$\tau_m(t) = J_m\ddot{\theta}_m(t) + f_m\dot{\theta}_m(t) \tag{2.30}$$

By using conservation of work that the work done by the beam is equal to the work done by the load related to motor it can be written as in Equation (2.31).

$$\tau_b^*(t) = \frac{\tau_b(t)\theta(t)}{\theta_m(t)} = n\tau_b(t) \tag{2.31}$$

By using Equation (2.27) and (2.29) together the Equation (2.32) is found as below.

$$\tau_b^*(t) = n^2\left[J_b\ddot{\theta}_m(t) + f_b\dot{\theta}_m(t)\right] \tag{2.32}$$

By using Equations (2.28), (2.30) and (2.32) , the torque developed by motor is found in Equation (2.33).

$$\begin{aligned}\tau(t) &= \tau_m(t) + \tau_b^*(t) = (J_m + n^2J_b)\ddot{\theta}_m(t) + (f_m + n^2f_b)\dot{\theta}_m(t)\\ &= J_{tot}\ddot{\theta}_m(t) + f_{eff}\dot{\theta}_m(t)\end{aligned} \tag{2.33}$$

where $J_{tot} = J_m + n^2J_b$ and $f_{eff} = f_m + n^2f_b$ is the effective viscous friction coefficent of the combined motor and load referred to the motor shaft.

Based on the results, the transfer function of single joint manipulator can be obtained. Because the torque created at the motor shaft increase linearly with the armature current as in the Equation (2.34), by using Kirchoff's voltage law the armature circuit Equation (2.35) can be used.

$$\tau(t) = K_a i_a(t) \tag{2.34}$$

$$V_a(t) = R_a i_a(t) + L_a \frac{di_a(t)}{dt} + e_b(t) \tag{2.35}$$

where e_b shown in Equation (2.36) is the back electromotive force (emf) that is proportional to the angular velocity of the motor and K_b is a proportionality constant in V.s/rad.

$$e_b(t) = K_b \dot{\theta}_m(t) \tag{2.36}$$

By taking the Laplace transform of the Equation (2.35) and using Equation (2.36) in this, the Equation (2.37) is obtained as below.

$$I_a(s) = \frac{V_a(s) - sK_b\theta_m(s)}{R_a + sL_a} \tag{2.37}$$

Taking the Laplace transform of the Equation (2.33), the Equation (2.38) is getted. Also, taking the Laplace transform of Equation (2.34) and using the Equation (2.37) it is found as in Equation (2.39).

$$T(s) = s^2 J_{tot}\theta_m(s) + sf_{eff}\theta_m(s) \tag{2.38}$$

$$T(s) = K_a I_a(s) = K_a \left[\frac{V_a(s) - sK_b\theta_m(s)}{R_a + sL_a} \right] \tag{2.39}$$

By rearranging the Equations (2.38) and (2.39) the transfer function from the armature voltage to the angular displacement is obtained in Equation (2.40).

$$\frac{\theta_m(s)}{V_a(s)} = \frac{K_a}{s\left[s^2 J_{tot}L_a + (L_a f_{eff} + R_a J_{tot})s + R_a f_{eff} + K_a K_b\right]} \tag{2.40}$$

Because the electrical time constant of the motor is much smaller than the mechanical time constant, the armature inductance effect, L_a can be ignored so that the Equation (2.41) is used.

$$\frac{\tau_m(s)}{V_a(s)} = \frac{K_a}{s\left[sR_aJ_{tot} + R_af_{eff} + K_aK_b\right]} = \frac{K}{s(T_ms+1)} \qquad \textbf{(2.41)}$$

where K and T_m are as in Equations (2.42a) and (2.42b).

$$K \triangleq \frac{K_a}{R_af_{eff} + K_aK_b} \qquad \text{motor gain constant} \qquad \textbf{(2.42a)}$$

$$T_m \triangleq \frac{R_aJ_{tot}}{R_af_{eff} + K_aK_b} \qquad \text{motor time constant} \qquad \textbf{(2.42b)}$$

Because the output of the control system is the angular displacement of the joint $\theta(s)$, by taking Laplace transform of the Equation (2.26) the transfer function of the single-joint manipulator relating the applied voltage to the angular displacement of the joint is getted as in Equation (2.43) and the block diagram is shown in Figure 2.21 by neglecting f_{eff} as drawn in **Fu and Gonzales (1987)**.

$$\frac{\theta(s)}{V_a(s)} = \frac{nK_a}{s\left[sR_aJ_{tot} + R_af_{eff} + K_aK_b\right]} \qquad \textbf{(2.43)}$$

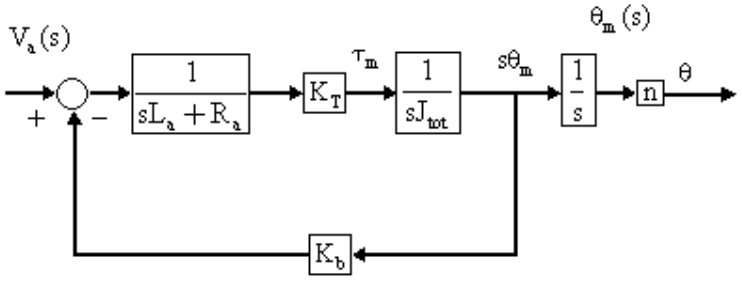


Figure 2.21: Open-loop transfer function of a single-joint robot arm

2.10.2 Positional controller for a single joint

The main idea of a positional controller is to servo the motor. Therefore, the actual angular displacement of the joint tracks a desired angular displacement which is defined by a preplanned trajectory. The technique is based on using the error signal given in Equation (2.44) between the desired and actual angular positions of the joint to actuate a suitable voltage.

$$V_a(t) = \frac{K_pe(t)}{n} = \frac{K_p\left[\theta_d(t) - \theta(t)\right]}{n} \qquad \textbf{(2.44)}$$

Here K_p is the position feedback gain in volts per radian, $e(t) = \theta_d(t) - \theta(t)$ is the system error, and n is the gear ratio. The Equation (2.44) shows that the actual angular displacement of the joint is fed back to obtain the error that is amplified with position feedback gain to get the applied voltage. By taking the Laplace transform of Equation (2.44) it is obtained as in Equation (2.45).

$$V_a(s) = \frac{K_p E(s)}{n} = \frac{K_p\left[\theta_d(s) - \theta(s)\right]}{n} \tag{2.45}$$

and substituing $V_a(s)$ into Equation (2.43), the open-loop transfer function relating the error actuating signal $\left[E(s)\right]$ to the actual displacement of the joint can be defined as in Equation (2.46).

$$\frac{\theta(s)}{\theta_d(s)} = \frac{G(s)}{1+1*G(s)} = \frac{K_a K_p}{s^2 R_a J_{tot} + s(R_a f_{eff} + K_a K_b) + K_a K_p} \tag{2.46}$$

By using forward path transfer function $G(s)$, the closed-loop transfer function relating the actual angular displacement $\theta(s)$ to the desired angular displacement $\theta_d(s)$ is found as in Equation (2.47).

$$\begin{aligned}\frac{\theta(s)}{\theta_d(s)} &= \frac{G(s)}{1+1*G(s)} = \frac{K_a K_p}{s^2 R_a J_{tot} + s(R_a f_{eff} + K_a K_b) + K_a K_p} \\ &= \frac{K_a K_p / R_a J_{tot}}{s^2 + \left[((R_a f_{eff} + K_a K_b)/R_a J_{tot}\right] s + K_a K_p / R_a J_{tot}}\end{aligned} \tag{2.47}$$

To increase the system response time and reduce the steady-state error, some damping into the system by adding a derivative of the positional error can be incorporated. By this added feedback, the applied voltage to the this joint motor is linearly proportional to the position error and its derivative as in Equation (2.48).The block diagram can be drawn by ignoring f_{eff} as in Figure 2.22 as defined by **Fu and Gonzalez (1987)**.

$$V_a(t) = \frac{K_p e(t) + K_d \dot{e}(t)}{n} = \frac{K_p\left[\theta_d(t) - \theta(t)\right] + K_d\left[\dot{\theta}_d(t) - \dot{\theta}(t)\right]}{n} \tag{2.48}$$

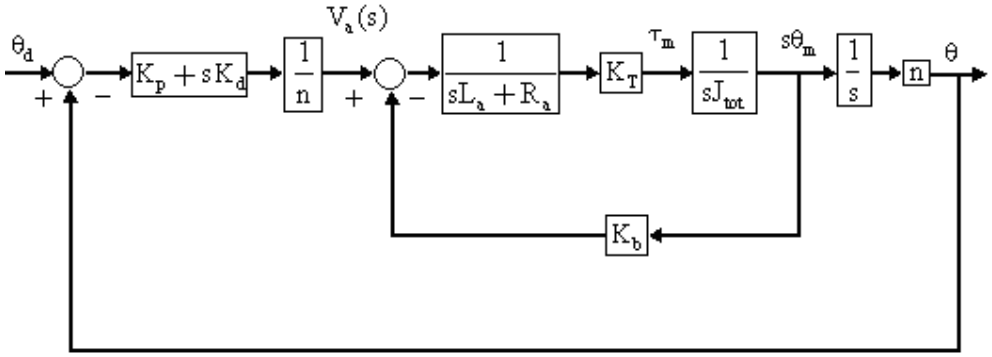


Figure 2.22: Feedback control of a single-joint manipulator

3. BEAM FORMULATIONS

In this chapter, equation of motions for both non-rotating and rotating clamped-free beams with beam theory of Euler-Bernoulli are found. For derivation of formulations Newton approach is used. Also, the boundary conditions of clamped-free beam are used.

3.1 Assumptions for Euler - Bernoulli Beam Theory

The assumptions made for modeling Euler-Bernoulli beam are as in below:

a. As in Figure 3.1 (a) rotation angle of beam element is very smaller than the bending deflection.

b. Deformations based on shear are very smaller than bending deformations.

c. By defining beam thickness as h and beam lenght as L, the ratio of h/L is very small ($h/L \leq 0.1$).

d. There is no twisting on beam due to the bending.

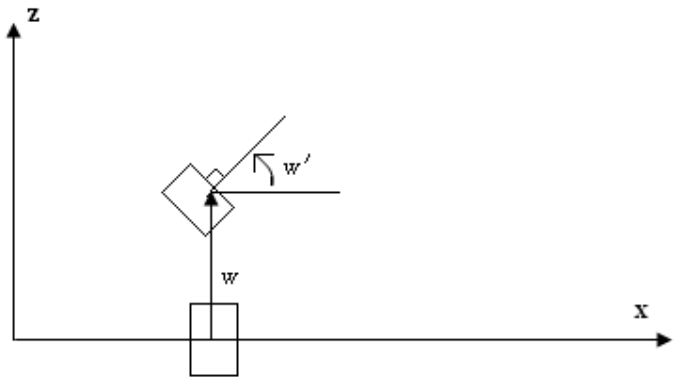


Figure 3.1 : Out of plane bending and rotation angle due to bending for Euler-Bernoulli beam element

3.2 Bending Motion of Non-rotating Uniform Euler-Bernoulli Beam

By using forces and moments as in Figure 3.2, equation of motion for a non-rotating, uniform, clamped-free Euler-Bernoulli beam can be found.

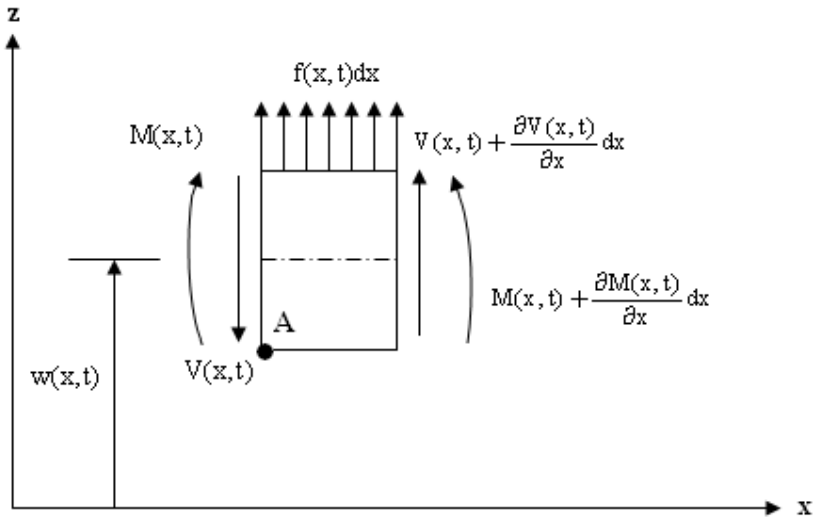


Figure 3.2 : Forces and moments acting on a non-rotating Euler-Bernoulli Beam

By using forces and moments equilibrium of moment for point A can be written as in Equation (3.1) taking counter-clockwise as positive way.

$$M(x,t)+\frac{\partial M(x,t)}{\partial x}dx-M(x,t)+\left[V(x,t)+\frac{\partial V(x,t)}{\partial x}dx\right]dx+f(x,t)dx\frac{dx}{2}=0 \quad \textbf{(3.1)}$$

After making necessary arrangements and dividing Equation (3.1) by dx and applying limit of $dx\rightarrow 0$, the Equation (3.2) can be found.

$$\frac{\partial M(x,t)}{\partial x}+V(x,t)=0 \quad \textbf{(3.2)}$$

By using forces in Figure 3.1 and taking z direction as positive way equilibrium of vertical force can be written as in Equation (3.3).

$$V(x,t)+\frac{\partial V(x,t)}{\partial x}dx-V(x,t)+f(x,t)dx=m(x)dx\frac{\partial^2 w(x,t)}{\partial t^2} \quad \textbf{(3.3)}$$

After making necessary arrangements and dividing Equation (3.3) by dx , the Equation (3.4) can be found.

$$\frac{\partial V(x,t)}{\partial x}+f(x,t)=m(x)\frac{\partial^2 w}{\partial t^2} \quad \textbf{(3.4)}$$

By using V(x,t) which is in the Equation (3.2) with Equation (3.4) principals of equation of motion can be written.

$$m(x)\frac{\partial^2 w(x,t)}{\partial t^2}+\frac{\partial^2 M(x,t)}{\partial x^2}=f(x,t) \qquad \textbf{(3.5)}$$

Also, the relation between the bending moment and beam deflection can be defined as below:

$$M(x,t)=EI(x)\frac{\partial^2 w}{\partial x^2}(x,t) \qquad \textbf{(3.6)}$$

If the Equation (3.6) is written in Equation (3.5), the equation of motion for a non-rotating Euler-Bernoulli beam is found with Newton approach as below:

$$m(x)\frac{\partial^2 w(x,t)}{\partial t^2}+\frac{\partial^2}{\partial x^2}\left[EI(x)\frac{\partial^2 w(x,t)}{\partial x^2}\right]=f(x,t), \qquad 0<x<L \qquad \textbf{(3.7)}$$

Since in this part free vibration analysis is done, $f(x,t)=0$ can be used.

3.3 Bending Motion of Rotating Uniform Euler-Bernoulli Beam

By using forces and moments as in Figure 3.3, equation of motion for a rotating, uniform, clamped-free Euler-Bernoulli beam can be found.

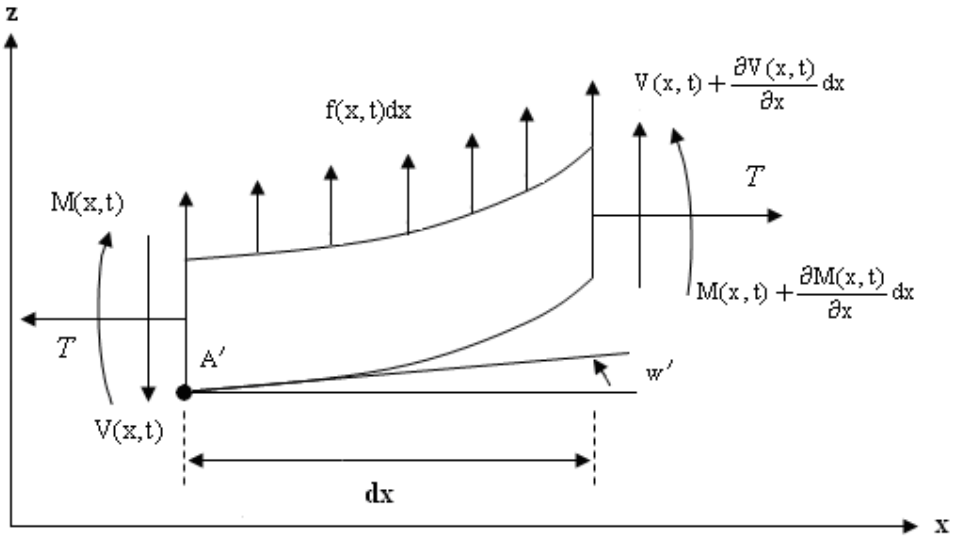


Figure 3.3 : Forces and moments acting on a rotating Euler-Bernoulli Beam

By using forces and moments equilibrium of moment for point A' can be written as in Equation (3.8) taking counter-clockwise as positive way.

$$M(x,t)+\frac{\partial M(x,t)}{\partial x}dx-M(x,t)+\left[V(x,t)+\frac{\partial V(x,t)}{\partial x}dx\right]dx+f(x,t)dx\frac{dx}{2}- \quad \textbf{(3.8)}$$
$$T\frac{\partial w}{\partial x}dx=0$$

After making necessary arrangements and dividing Equation (3.8) by dx and applying limit of dx→0 , the Equation (3.9) can be found.

$$V(x,t)=T\frac{\partial w}{\partial x}-\frac{\partial M(x,t)}{\partial x} \quad \textbf{(3.9)}$$

By using forces in Figure 3.2 and taking z direction as positive way equilibrium of vertical force can be written as in Equation (3.10).

$$V(x,t)+\frac{\partial V(x,t)}{\partial x}dx-V(x,t)+f(x,t)dx=m(x)dx\frac{\partial^2 w(x,t)}{\partial t^2} \quad \textbf{(3.10)}$$

After making necessary arrangements and dividing Equation (3.10) by dx , the Equation (3.11) can be found.

$$\frac{\partial V(x,t)}{\partial x}+f(x,t)=m(x)\frac{\partial^2 w}{\partial t^2} \quad \textbf{(3.11)}$$

If the Equations (3.6) and (3.9) are written in Equation (3.11), the equation of motion for a rotating Euler-Bernoulli beam is found with Newton approach as below:

$$m(x)\frac{\partial^2 w(x,t)}{\partial t^2}+\frac{\partial^2}{\partial x^2}\left[EI(x)\frac{\partial^2 w(x,t)}{\partial x^2}\right]-\frac{\partial}{\partial x}\left[T\frac{\partial w(x,t)}{\partial x}\right]=f(x,t) \quad \textbf{(3.12)}$$

3.4 Centrifugal Force

Centrifugal force is important term for rotating beam equations and this term is tendency of leave of rotating axis for a rotating beam around a point. In this section, derivation of centrifugal force is done. In Figure 3.4 there is a uniform beam rotating with a fixed rotation speed Ω , having rotor diameter of R and clamped-free at point O. Also, it has homogenous and isotropic material property.

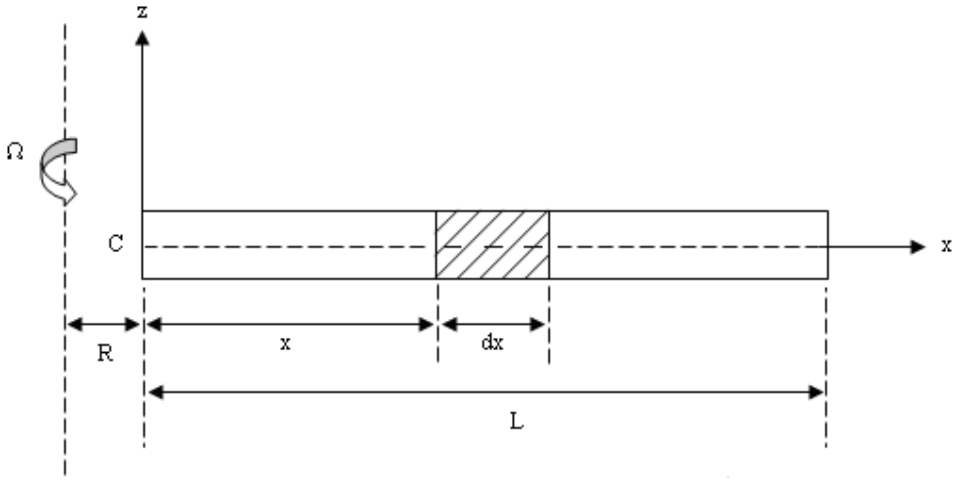


Figure 3.4 : Rotating, uniform, clamped-free beam model

Here, a beam element having lenght of dx is taken and it is examined in Figure 3.5. Also, the equilibrium equation for x direction is written to obtain centrifugal force.

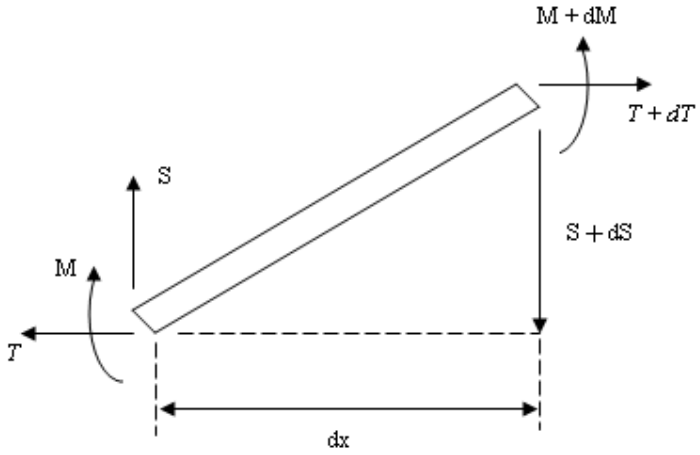


Figure 3.5 : Forces and moments acting on a rotating beam element

The speed of a beam element as seen in Figure 3.4 can be written as below:

$$V = \Omega(R + x) \tag{3.30}$$

By using Equation (3.30) the centrifugal force acting on beam element is defined as in Equation (3.31).

$$F_C = \frac{mV^2}{(R+x)} = m\Omega^2(R + x) \tag{3.31}$$

Also by writing forces acting on beam element for x direction the pull force can be found.

$$T + dT - T = m\Omega^2(R + x)dx \quad \longrightarrow \quad dT = m\Omega^2(R + x)dx \tag{3.32}$$

By taking integral of Equation (3.32) the pull force acting on whole beam can be obtained.

$$T = \int_0^L m\Omega^2(R + x)dx \tag{3.33}$$

4. DIFFERENTIAL TRANSFORM METHOD

4.1 History

Firstly, the differential transform method was used for analysis of electric circuits, and linear-nonlinear initial boundary problems by **Zhou (1986)**. Also, **Chiou and Tzeng (1996)** used Taylor transformation for the solution of nonlinear vibration problems. Since this method can be used for both ordinary and partial differential equations, **Jang (2001)** used two dimensional differential transform method in order to solve partial differential equations. Moreover, **Abdel and Hassan (2002)** used this method for the solution of eigenvalue problems. Shortly, in the preceding studies differential transform method has been used widely for the solution of nonlinear or variable parameter problems.

4.2 Definition of Method

Differential Transform Method depends on Taylor series expansion and is used for the analytic solution of differential equations. In this method, transformation rules are applied for the differential equations and boundary conditions and simple analytic expressions are gotten. After that, by solving these expressions the desired results are obtained with high accuracy.

In the region of D if $f(x)$ is an analytic function and x_0 is in the this region , $f(x)$ can be written by series expansion near $x= x_0$ as

$$f(x)=\sum_{k=0}^{\infty}\frac{(x-x_0)^k}{k!}\left(\frac{d^k}{dx^k}\right)_{x=x_0} \qquad \textbf{(4.1)}$$

Here, $f(x)$ is the original function . Also, the differential transform of this function can be defined as below by using the transformed function $F[k]$.

$$F[k]=\frac{1}{k!}\left(\frac{d^k f(x)}{dx^k}\right)_{x=x_0} \qquad \textbf{(4.2)}$$

By using Equations (3.1) and (3.2) together, the relation between origianl and transformed function can be found.

$$f(x)=\sum_{k=0}^{\infty}\frac{(x-x_0)^k}{k!}F(k) \tag{4.3}$$

In this series expansion method taking finite number of terms is a general approach. Therefore, the Equation (3.3) is written with the finite number of q. Here, q defines the convergence speed.

$$f(x)=\sum_{k=0}^{q}\frac{(x-x_0)^k}{k!}F(k) \tag{4.4}$$

4.3 Application of Method

The theorems used for the transformations of differential equations are written below.

Theorem 4.1:

$$f(x)=g(x)\pm h(x) \quad \Rightarrow \quad F[k]=G[k]\pm H[k] \tag{4.5a}$$

Theorem 4.2:

$$f(x)=\lambda g(x) \quad \Rightarrow \quad F[k]=\lambda G[k] \tag{4.5b}$$

Theorem 4.3:

$$f(x)=g(x)h(x) \quad \Rightarrow \quad F[k]=\sum_{l=0}^{k}G[k-l]\,H[l] \tag{4.5c}$$

Theorem 4.4:

$$f(x)=\left[g_1(x)g_2(x).....g_{n-1}(x)g_n(x)\right] \quad \Rightarrow$$

$$F[k]=\sum_{k_{n-1}=0}^{k}\sum_{k_{n-2}=0}^{k_{n-1}}.....\sum_{k_2=0}^{k_3}\sum_{k_1=0}^{k_2}G_1(k_1)G_2(k_2-k_1)....G_{n-1}(k_{n-1}-k_{n-2})G_n(k-k_{n-1}) \tag{4.5d}$$

Theorem 4.5:

$$f(x)=\frac{d^n g(x)}{dx^n} \quad \Rightarrow \quad F[k]=\frac{(k+n)!}{k!}G[k+n] \tag{4.5e}$$

Theorem 4.6:

$$f(x)=x^{n} \qquad \Rightarrow \qquad F[k]=\delta(k-n)=\begin{cases}0 & \text{if } k\neq n\\ 1 & \text{if } k=n\end{cases} \tag{4.5f}$$

Theorem 4.7:

$$f(x)=\left[g_1(x)g_2(x).....g_{n-1}(x)g_n(x)\right]\int_{x_0}^{x} h_1(t)h_2(t).....h_{m-1}(t)h_m(t)dt \quad \Rightarrow$$

$$F[k]=\sum_{k_{m+n-1}=0}^{k}\ \sum_{k_{m+n-2}=0}^{k_{m+n-1}} .....\sum_{k_2=0}^{k_3}\ \sum_{k_1=0}^{k_2}\frac{1}{k_m}H_1\left[k_1-1\right]H_2\left[k_2-k_1\right].....H_{m-1}\left[k_{m-1}-k_{m-2}\right]$$

$$xG_1\left[k_{m+1}-k_m\right]G_2\left[k_{m+2}-k_{m+1}\right].....G_{n-1}\left[k_{m+n-1}-k_{m+n-2}\right]G_n\left[k-k_{m+n-1}\right] \tag{4.5g}$$

The theorems used for the transformation of boundary conditions are listed at Table 4.1.

Table 4.1: Differential transformations of boundary conditions

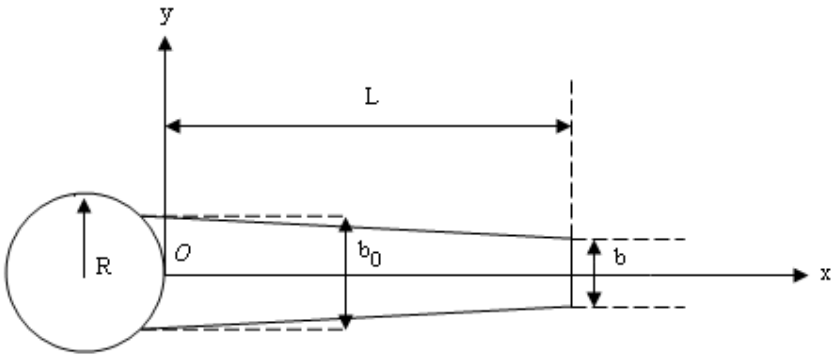
x=0		x=1	
Original Boundary Condition	**Transformed Boundary Condition**	**Original Boundary Condition**	**Transformed Boundary Condition**
$f(0)=0$	$F[0]=0$	$f(1)=0$	$\sum_{k=0}^{\infty}F[k]=0$
$\frac{df(0)}{dx}=0$	$F[1]=0$	$\frac{df(1)}{dx}=0$	$\sum_{k=0}^{\infty}kF[k]=0$
$\frac{d^2f(0)}{dx^2}=0$	$F[2]=0$	$\frac{d^2f(1)}{dx^2}=0$	$\sum_{k=0}^{\infty}(k-1)kF[k]=0$
$\frac{d^3f(0)}{dx^3}=0$	$F[3]=0$	$\frac{d^3f(1)}{dx^3}=0$	$\sum_{k=0}^{\infty}(k-2)(k-1)kF[k]=0$

5. VIBRATION ANALYSIS OF ROTATING TAPERED BEAMS

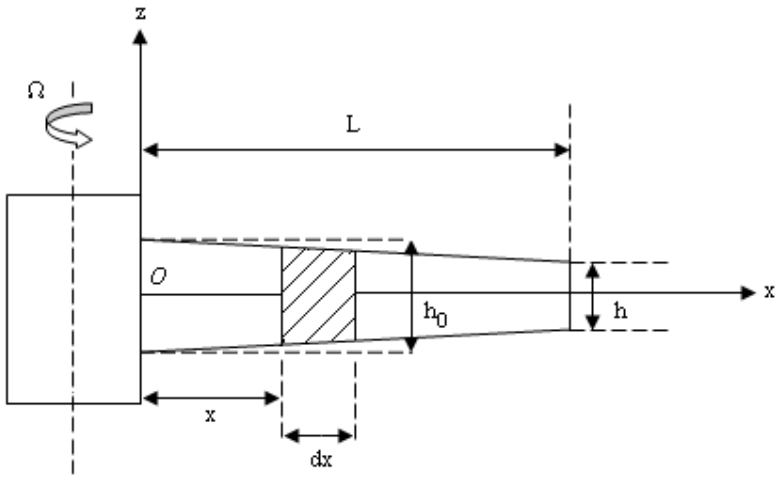
In this part, the vibration analysis of rotating tapered Euler-Bernoulli beam is done. Derivation of equation of motion and boundary conditions are examined in part 3.3 detailly for the untapered situation. Also, solution of the equation of motion are obtained by using Differential Transform Method (DTM). Moreover, the effects of taper ratio, rotation speed and rotor shaft diameter on the vibration parameters are found.

5.1 Beam Model

The beam model used in this study is shown in Figure 5.1. In this Figure Ω is the rotation speed, R is the rotor diameter, and L is the lenght of Euler-Bernoulli beam. The beam goes h_0 to h in xz plane and b_0 to b in xy plane. In the used cartesian coordinate system x axis is on the undeformed neutral axis and z axis is not on the rotation axis. Also, z axis is parallel to rotation axis. Morover, y axis is in the rotation plane. Therefore, principal axes of the beam are parallel to y and z axes. Also, the beam examined in this study is both isotropic and having symmetric cross-section by two principal axes. Therefore, for all cross-sections elastic axes are on the center of mass. Also, bending vibration is not related to twisting vibration.



(a)



(b)

Figure 5.1 : Double tapered Euler-Bernoulli beam **(a)** Top view **(b)** Lateral view

5.2 Equation of Motion and Boundary Conditions

Equation of motion for rotating, uniform Euler-Bernoulli beam is derived in part 3.2.3.

$$\rho A\frac{\partial^2 w}{\partial t^2}+\frac{\partial^2}{\partial x^2}\left(EI\frac{\partial^2 w}{\partial x^2}\right)-\frac{\partial}{\partial x}\left(T\frac{\partial w}{\partial x}\right)=p_w \qquad \textbf{(5.1)}$$

Since free-vibration analysis is done, p_w is taken as zero. Also, centrifugal force *T* is as in Equation (3.33). Moreover, boundary conditions for clamped-free Euler-Bernoulli beam can be written as below

$$\text{For } x=0 \quad \rightarrow \quad w=0 \text{ and } \frac{\partial w}{\partial x}=0 \qquad \textbf{(5.2a)}$$

$$\text{For } x=L \quad \rightarrow \quad \frac{\partial^2 w}{\partial x^2}=0 \text{ and } \frac{\partial^3 w}{\partial x^3}=0 \qquad \textbf{(5.2b)}$$

To find solution of equation of motion in Equation (5.1) assumption of simple harmonic motion is done and out of plane bending deflection w(x,t) is defined as below:

$$w(x,t)=\bar{w}(x)e^{i\omega t} \qquad \textbf{(5.3)}$$

Also, by using this term in Equation (5.1) the equation of motion can be found.

$$\omega^2 \rho A \bar{w} - \frac{d^2}{dx^2} - \frac{d^2}{dx^2}\left(EI\frac{d^2\bar{w}}{dx^2}\right) + \frac{d}{dx}\left(T\frac{d\bar{w}}{dx}\right) = 0 \qquad \textbf{(5.4)}$$

5.3 Tapered Beam Formulations and Nondimensional Parameters

For a double tapered beam the beam lenght b(x), beam thickness h(x), cross-section area A(x) and area moment of inertia I(x) can be written as below:

$$b(x) = b_0\left(1 - c_b\frac{x}{L}\right)^m \qquad \textbf{(5.5a)}$$

$$h(x) = h_0\left(1 - c_h\frac{x}{L}\right)^n \qquad \textbf{(5.5b)}$$

$$A(x) = A_0\left(1 - c_b\frac{x}{L}\right)^m\left(1 - c_h\frac{x}{L}\right)^n \qquad \textbf{(5.5c)}$$

$$I(x) = I_0\left(1 - c_b\frac{x}{L}\right)^m\left(1 - c_h\frac{x}{L}\right)^{3n} \qquad \textbf{(5.5d)}$$

Here, bottom indice $(\ )_0$ defines the values connected to beam root. For example, if the beam is taken as linear as in this study, n=1 and m=1 values can be used. Also, wideness taper ratio c_b, thickness taper ratio c_h, root cross-section area $A_0(x)$ and root moment of inertia $I_0(x)$ can be defined as below:

$$c_b = \left(1 - \frac{b}{b_0}\right) \qquad \textbf{(5.6a)}$$

$$c_h = \left(1 - \frac{h}{h_0}\right) \qquad \textbf{(5.6b)}$$

$$A_0 = b_0 h_0 \qquad \textbf{(5.7a)}$$

$$I_0 = \frac{b_0 h_0^3}{12} \qquad \textbf{(5.7b)}$$

In this study modulus of elasticity E, shear modulus G, and material density ρ is constant in whole beam. Also, mass per lenght ρA and bending rigidity EI change as

in Equations (5.5c) and (5.5d). To simplify equations nondimensional parameters are defined as below:

$$\xi = \frac{x}{L}, \quad \delta = \frac{R}{L}, \quad \tilde{w}(\xi) = \frac{\bar{w}}{L}, \quad \eta^2 = \frac{\rho A_0 L^4 \Omega^2}{EI_0}, \quad \mu^2 = \frac{\rho A_0 L^4 \omega^2}{EI_0} \tag{5.8}$$

By using nondimensional parameters and tapered beam formulations in Equation (3.33) the nondimensional centrifugal force is obtained. Also, by using these terms in Equation (5.4) the nondimensional equation of motion for linear situation (m=1, n=1) can be found as below:

$$\frac{d^2}{d\xi^2}\left[(1-c_b\xi)(1-c_h\xi)^3\frac{d^2\hat{w}}{d\xi^2}\right] - \mu^2(1-c_b\xi)(1-c_h\xi)\hat{w} - \eta^2\frac{d}{d\xi}\left\{\left[\frac{c_b c_h}{4}(1-\xi^4)+\delta(1-\xi)\right.\right.$$
$$\left.\left.+\frac{1}{2}(1-c_b\delta-c_h\delta)(1-\xi^2)+\frac{1}{3}(-c_b-c_h+c_b c_h\delta(1-\xi^3)\right]\frac{d\hat{w}}{d\xi}\right\} = 0 \tag{5.9}$$

Also, the boundary conditions given in Equations (5.2a) and (5.2b) can be written as nondimensional as below:

$$\text{For} \quad \xi = 0 \quad \rightarrow \quad \hat{w} = 0 \quad \text{and} \quad \frac{d\hat{w}}{d\xi} = 0 \tag{5.10a}$$

$$\text{For} \quad \xi = 1 \quad \rightarrow \quad \frac{d^2\hat{w}}{d\xi^2} = 0 \quad \text{and} \quad \frac{d^3\hat{w}}{d\xi^3} = 0 \tag{5.10b}$$

5.4 Application of Differential Transform Method

By using Differential Transform Method mentioned in Chapter 4 in Equation (5.9) transformed equation can be found as below:

$$(k+1)(k+2)(k+3)(k+4)W[k+4] - [(k+1)(k+2)^2(k+3)(c_b+3c_h)]W[k+3] +$$
$$(k+1)(k+2)\left\{3c_h(c_b+c_h)(k+1)(k+2)+\eta^2\left[\frac{1}{2}(c_b\delta+c_h\delta-1)+\frac{1}{3}(c_b\delta+c_h-c_b c_h\delta)-\right.\right.$$
$$\left.\left.\frac{1}{4}c_b c_h\delta\right]\right\}W[k+2] + \left[(k+1)^2\delta\eta^2 - c_h^2(3c_b+c_h)(k-2)(k-1)k(k+1)\right]W[k+1] +$$
$$(k+1)\left[c_b c_h^3 k(k+1)(k+2)+\frac{1}{2}(1-c_b\delta-c_h\delta)k\eta^2-\mu^2\right]W[k] + \left[(c_b+c_h)\mu^2 +\right.$$
$$\left.\frac{1}{3}(c_b c_h\delta-c_b-c_h)(k-1)(k+1)\right]W[k-1] + \left[\frac{c_b c_h}{4}(k+1)(k-2)\eta^2 - c_b c_h\eta^2\right]W[k-2] = 0 \tag{5.11}$$

Also, by using Differential Transform Method in Equations (5.10a) and (5.10b) transformed boundary conditions can be obtained.

For $\xi = 0 \quad \rightarrow \quad W[0] = 0 \quad \text{and} \quad W[1] = 0$ **(5.12a)**

For $\xi = 1 \quad \rightarrow \quad \sum_{k=2}^{\infty} k(k-1)W[k] = 0 \quad \text{and} \quad \sum_{k=3}^{\infty} k(k-1)(k-2)W[k] = 0$ **(5.12b)**

6. VIBRATION CONTROL OF ROTATING STRUCTURES

6.1 Governing Equations of Rotating Euler-Bernoulli Beam

The motion of an Euler-Bernaulli beam is examined in this part and is shown in Figure 6.1 as in **Zhu and Mote (1997)**. Here there is no gravitational force.The transverse displacement of the beam at the point P on the x axis is denoted by w(x,t) and longitudinal deformation of the beam is not considered.

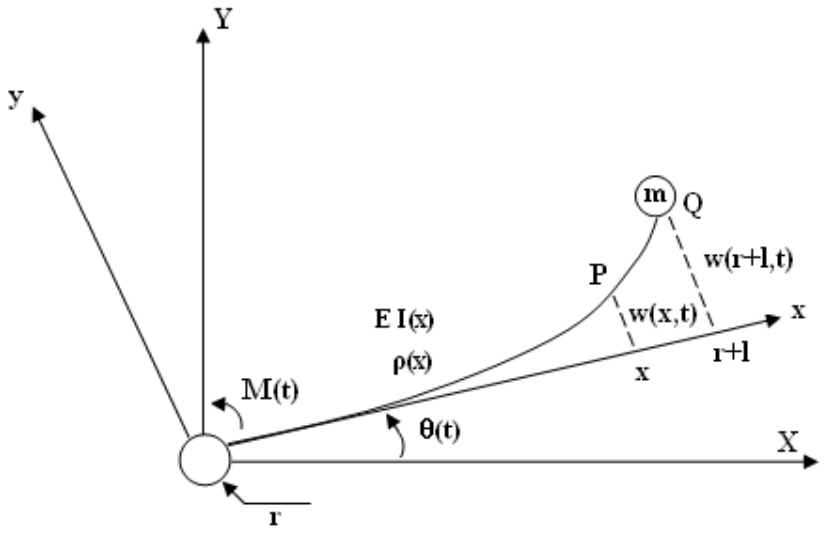


Figure 6.1 : Euler-Bernaulli beam with end mass attached to a rigid hub

The inertial velocity of the point P on the beam can be written with displacement as in Equation (6.1).

$$v_P = -w(x,t)\dot{\theta}(t)e_1 + (x\dot{\theta} + w_t(x,t))e_2 \qquad \textbf{(6.1)}$$

where e_1 and e_2 are the unit vectors along the x and y axies, respectively. The kinetic energy is as in Equation (6.2).

$$T = \frac{1}{2} I_m \ddot{\theta}^2 + \frac{1}{2} \int_r^{r+\ell} \rho(x) v_P . v_P dx + \frac{1}{2} \boldsymbol{m} v_Q . v_Q$$

$$= \frac{1}{2} I_m \ddot{\theta}^2 + \frac{1}{2} \int_r^{r+\ell} \rho(x)(w^2\dot{\theta}^2 + x^2\dot{\theta}^2 + w_t^2 + w_t^2 + 2x\dot{\theta}w_t)dx + \frac{1}{2}\boldsymbol{m}\Big[w^2(r+\ell,t)\dot{\theta}^2 + \quad \textbf{(6.2)}$$
$$(r+\ell)^2\dot{\theta}^2 + w_t^2(r+\ell,t) + 2(r+\ell)\dot{\theta}\, w_t(r+\ell,t)\Big]$$

where v_Q is stated in Equation (6.3).

$$v_Q = v_P(r+\ell,t) \quad \textbf{(6.3)}$$

The potential energy expression including both the bending energy and the work done by the axial centrifugal force F(x,t) can be obtained as in Equation (6.4).

$$V = \frac{1}{2} \int_r^{r+\ell} EI(x) w_{xx}^2 dx + \frac{1}{2} \int_r^{r+\ell} F(x,t) w_x^2 dx \quad \textbf{(6.4)}$$

and F(x,t) can be used as in Equation (6.5)

$$F(x,t) = \int_x^{r+\ell} \rho(\xi)\dot{\theta}^2 \xi d\xi + m(r+\ell)\dot{\theta}^2 \quad \textbf{(6.5)}$$

The virtual work done by the external moment M(t) is as in Equation (6.6).

$$\delta W = M(t)\delta\theta \quad \textbf{(6.6)}$$

By substituting Equations (6.2) and (6.4) into the extended Hamilton's principle shown in Equation (6.7), applying the variational operation and integration by parts and neglecting terms of higher order in w yields Equations (6.8) and (6.9) describing $\theta(t)$ and w(x,t).

$$\int_{t_1}^{t_2} (\delta T - \delta V + \delta W)dt = 0 \quad \textbf{(6.7)}$$

$$(I_m + I_b)\ddot{\theta} + \int_r^{r+\ell} \rho(x) x w_{tt} dx + \boldsymbol{m}(r+\ell) w_{tt}(r+\ell,t) = M(t) \quad \textbf{(6.8)}$$

$$\rho(x)w_{tt}+[EI(x)w_{xx}]_{xx}=\dot{\theta}^2 w_{xx}\int_x^{r+\ell}\rho(\xi)\xi d\xi-\dot{\theta}^2\rho(x)x-\dot{\theta}^2(xw_x-w)\rho(x) \quad \textbf{(6.9)}$$

$$+m(r+\ell)\dot{\theta}^2 w_{xx}$$

where I_b is the moment of inertia of the deformed beam with end-mass about the z-axis as in Equation (6.10).

$$I_b=\int_r^{r+\ell}\rho(x)x^2dx+m(r+\ell)^2 \quad \textbf{(6.10)}$$

The boundary conditions are shown in Equations (6.11), (6.12), (6.13) and (6.14).

$$w(x,t)\big|_{x=r}=0 \quad \textbf{(6.11)}$$

$$w_x(x,t)\big|_{x=r}=0 \quad \textbf{(6.12)}$$

$$w_{xx}(x,t)\big|_{x=r+\ell}=0 \quad \textbf{(6.13)}$$

$$\left[EI(x)w_{xx}(x,t)\right]_x\big|_{x=r+\ell}=\boldsymbol{m}\{w_{tt}(r+\ell,t)+(r+\ell)\ddot{\theta}+\dot{\theta}^2[(r+\ell)w_x(r+\ell,t)-w(r+\ell,t)]\} \quad \textbf{(6.14)}$$

By using that the terms multiplied $\dot{\theta}^2$ are ignored so that centrifugal force is eliminated, the Equations (6.9) and (6.14) are turn into Equations (6.15) and (6.16).

$$\rho(x)w_{tt}+[EI(x)w_{xx}]_{xx}=-x\ddot{\theta}\rho(x) \quad \textbf{(6.15)}$$

$$[EI(x)w_{xx}(x,t)]_x\big|_{x=r+\ell}=\boldsymbol{m}[w_{tt}(r+\ell,t)+(r+\ell)\ddot{\theta}] \quad \textbf{(6.16)}$$

By using the decoupling theorem defined in **Zhu and Mote (1997)** that the linear, coupled integro-differential Equations (6.8) and (6.15) and boundary conditions defined in Equations (6.11), (6.13) and (6.16) are equivalent to the Euler-Bernaulli beam equation shown in Equation (6.18) with boundary conditions obtained as in Equations (6.19), (6.20), (6.21) and (6.22) with the transformation in the Equation (6.17).

$$y(x,t)=w(x,t)+x\theta(t) \quad \textbf{(6.17)}$$

$$[EI(x)y_{xx}]_{xx}+\rho(x)y_{tt}=0 \quad \textbf{(6.18)}$$

$$y(r,t) = r y_x(r,t) \tag{6.19}$$

$$I_m y_{xtt}(r,t) + r[EI(x)y_{xx}]_x\big|_{x=r} - [EI(x)y_{xx}]\,\big|_{x=r} = M(t) \tag{6.20}$$

$$y_{xx}(r+\ell,t) = 0 \tag{6.21}$$

$$[EI(x)y_{xx}(x,t)]_x\big|_{x=r+\ell} = \boldsymbol{m} y_{rr}(r+\ell,t) \tag{6.22}$$

By Equations (6.11) and (6.12), y(r,t)=rθ(t) and $y_x(r,t) = \theta(t)$ leading to Equation (6.19) and the Equation (6.8) becomes as in Equation (6.23).

$$(I_m + I_b)\ddot{\theta} + \int_r^{r+\ell} \rho(x) x y_{tt}(x,t)dx + \boldsymbol{m}(r+\ell,t) = M(t) \tag{6.23}$$

In this master thesis, the model do not have tip mass and hub radius is ignored. Hence, the governing equations are found as in Equations (6.24) and (6.25).

$$EIw^{(4)} + m\ddot{w} = -mx\ddot{\theta} \tag{6.24}$$

$$J_{tot}\ddot{\theta} + \int_0^1 m\ddot{w}xdx = \tau \tag{6.25}$$

Also , J_{tot} that the total rotational inertia is used as in Equation (6.26).

$$J_{tot} = \frac{J_m}{n^2} + J_b \tag{6.26}$$

6.2 Structural Parameters For Rotating Euler-Bernoulli Beam

The sum of the orthogonal modes can be written as in Equation (6.27) defined in **Hodges and Pierce (2002)** and it can be also used for solving Equation (6.24).

$$w(t,x) = \sum_{i=1}^{n} \phi_i q_i(t) \tag{6.27}$$

Here $\phi_i(x)$ ith orthogonal mode and $q_i(t)$ is the ith generalized coordinate. The characteristic equation is as below in Equation (6.28).

$$\cosh\alpha_i\ell\cos\alpha_i\ell + 1 = 0 \tag{6.28}$$

where $\alpha_i\ell$ is as in Equation (6.29).

$$(\alpha_i \ell)^2 = \sqrt{\frac{m\ell^4}{EI}}\omega_i \tag{6.29}$$

and the ith orthogonal mode of the clamped-free beam can be given as below in Equation(6.30).

$$\phi_i = C\left[\cosh(\alpha_i x) - \cos(\alpha_i x) - \frac{\sinh(\alpha_i \ell) - \sin(\alpha_i \ell)}{\cosh(\alpha_i \ell) + \cos(\alpha_i \ell)}[\sinh(\alpha_i \ell) - \sin(\alpha_i x)]\right] \tag{6.30}$$

Here, ω_i is the ith natural frequency of the beam. By substituting Equation (6.27) in Equation (6.24) and using orthogonality conditions shown in Equations (6.31) and (6.32), the following Equation (6.33) is obtained.

$$\int \phi_i \phi_j dx = \int \phi_i^2 dx \ , \quad i = j \tag{6.31}$$

$$\int \phi_i \phi_j dx = 0 \ , \quad i \neq 0 \tag{6.32}$$

$$\ddot{q}_i + \omega_i^2 q_i = -\ell \varphi_i \ddot{\theta} \tag{6.33}$$

φ_i, ω_i and ξ are as in Equations (6.34), (6.35) and (6.36).

$$\varphi_i = \frac{\int_0^1 \xi \phi_i(\xi) d\xi}{\int_0^1 \phi_i^2(\xi) d\xi} \tag{6.34}$$

$$\omega_i = (\alpha_i \ell)^2 \sqrt{\frac{EI}{m\ell^4}} \tag{6.35}$$

$$\xi = \frac{x}{\ell} \tag{6.36}$$

Here φ_i is the mode participation factor. After taking Laplace transform of Equation (6.33), the resulting Equation (6.37) is found.

$$(s^2 + \omega_i^2)\bar{Q}_i(s) + s^2\theta(s) = 0 \tag{6.37}$$

where $\bar{Q}_i$ is as in Equation (6.38).

$$\bar{Q}_i(s) = \frac{Q_i(s)}{\ell \varphi_i} \tag{6.38}$$

By using the Equation (6.27) in Equation (6.25) it is found as in Equation (6.39).

$$\ddot{\theta}+\sum_{i=1}^{n}\eta_i\ddot{\bar{q}}_i=\frac{\tau}{J_{tot}} \tag{6.39}$$

Here η_i can be written as in Equation (6.40).

$$\eta_i=\frac{3\varphi_i\int_0^1\xi\phi_i(\xi)d\xi}{1+\frac{(J_m/n^2)}{J_b(1-\frac{3}{4}c_h)}} \tag{6.40}$$

where $\bar{q}_i$ and J_b are as in Equations (6.41) and (6.42).

$$\bar{q}_i=\frac{q_i}{\ell\varphi_i} \tag{6.41}$$

$$J_b=J_m/n^2 \tag{6.42}$$

6.3 Block Diagram of Model and Transfer Functions

The block diagram which is used to model this system is shown in Figure 6.2 modeled as in **Diken (1999)**. From this diagram the Laplace transform of torque with respect to beam axis is getted as in Equation (6.43).

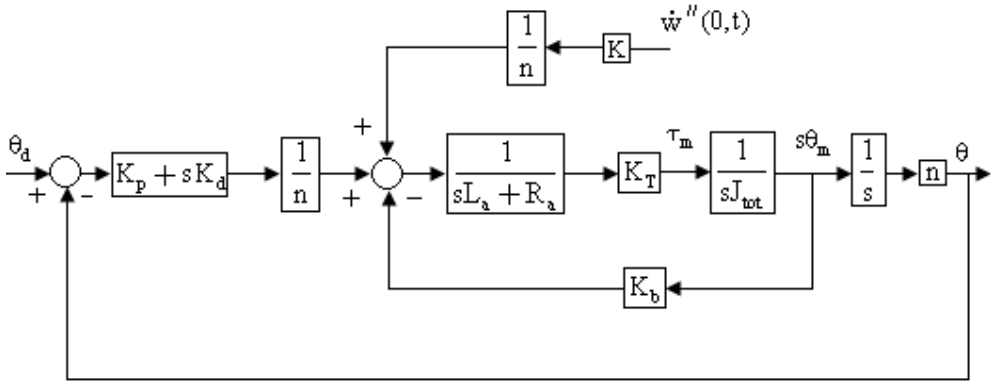


Figure 6.2 : Block diagram of servomotor control with shear strain feedback

$$T(s)=\frac{K_T}{n^2R_0}\left[\left[\theta_d(s)-\theta(s)\right](K_p+sK_d)-sK_b\theta(s)-sK\sum_{i=1}^{n}\phi_i''(0)\ell\varphi_i\bar{Q}_i(s)\right] \tag{6.43}$$

In this block diagram, K_T is the torque constant, R_a is the coil resistance, θ_d is the desired angular input, K_p is proportional gain, K_d is the derivative gain, K_b is the electromotive force constant and **K** is the shear strain feedback gain. The armature coil resistance R_a is mostly much greater than the armature coil inductance L_a so that L_a is ignored. By taking Laplace transform of Equation (6.39) and using Equation (6.43) , the resulting equation can be written as in Equation (6.44).

$$\left[\eta_1 s^2 - \ell\alpha_1 \phi_1''(0)\frac{K_T K}{n^2 J_{tot} R_a} s\right]\bar{Q}_1(s) + \left[s^2 + \frac{K_T\left[(K_d + K_b)s + K_p\right]}{n^2 J_{tot} R_a}\right]\theta(s) = \left[\frac{K_T(K_p + sK_d)}{n^2 J_{tot} R_a}\right]\theta_d(s) \qquad \textbf{(6.44)}$$

The parametric transfer functions relating the tip motion to the desired rotation and the beam rotation to the desired rotation are obtained by using Equations (6.39) and (6.44) as in the work of **Diken (1999)** with the difference that ζ_{s1} is proportional to $\phi_1''(0)$ instead of $\phi_1'''(0)$ because of using bending strain as a feedback and shown in Equations (6.45) and (6.46).

$$\frac{\bar{Q}_1(s)}{\theta_d(s)} = \frac{-s^2(2\zeta s + 1)}{(1-\eta_1)s^4 + 2\zeta(1+\gamma_1)s^3 + (\rho_1^2 + 1)s^2 + 2\zeta\rho_1^2 s + \rho_1^2} \qquad \textbf{(6.45)}$$

$$\frac{\theta(s)}{\theta_d(s)} = \frac{(s^2 + \rho_1^2)(2\zeta s + 1)}{(1-\eta_1)s^4 + 2\zeta(1+\gamma_1)s^3 + (\rho_1^2 + 1)s^2 + 2\zeta\rho_1^2 s + \rho_1^2} \qquad \textbf{(6.46)}$$

where

$$\rho_1 = \frac{\omega_1}{\omega}, \quad \gamma_1 = \frac{\zeta_{s1}}{\zeta}, \quad \omega^2 = \frac{K_T K_p}{n^2 J_{tot} R_a}, \quad 2\zeta_{s1}\omega = \ell\alpha_1 \phi_1''(0)\frac{K_T K}{n^2 J_{tot} R_a},$$

$$2\zeta\omega = \frac{K_T(K_d + K_b)}{n^2 J_{tot} R_a} \qquad \textbf{(6.47)}$$

Here, ρ_1 is the frequency ratio, ω is the control system frequency, ω_1 is the first natural frequency of the beam, ζ is the control system damping, ζ_{s1} is the damping ratio for the bending strain feedback and γ_1 is the ratio between these dampings. These parameters change with taper ratio as in Equation (6.48).

$$\rho_{1_2} = \rho_{1_1} \frac{\omega_{1_2}}{\omega_{1_1}} \sqrt{\frac{8-3c_{h2}}{8-3c_{h1}}}, \qquad \gamma_{1_2} = \gamma_{1_1} \frac{\alpha_{1_2}\phi_{1_2}''(0)}{\alpha_{1_1}\phi_{1_1}''(0)}, \qquad \omega_2 = \omega_1 \sqrt{\frac{8-3c_{h1}}{8-3c_{h2}}}$$

$$\zeta_2 = \zeta_1 \sqrt{\frac{8-3c_{h1}}{8-3c_{h2}}}, \qquad \zeta_{s1_2} = \zeta_{s1_1} \frac{\alpha_{1_2}\phi_{1_2}''(0)}{\alpha_{1_1}\phi_{1_1}''(0)} \sqrt{\frac{8-3c_{h1}}{8-3c_{h2}}} \tag{6.48}$$

where c_{h1} is the reference taper ratio that is used for a uniform beam and takes the zero value. The other nonzero taper ratios that are used for tapered beams are represented by c_{h2}.

In Table 6.1, effect of the taper ratio on the beam parameters is given. Here the fundamental frequency is calculated and compared with the frequency values that take place in the work of **Ozdemir and Kaya (2006)** for validation. When the results are compared, it is seen that there is a good agreement between the results.

Table 6.1: Effect of taper ratio on beam parameters

c_h	ω_1	**Ozdemir and Kaya (2006)**	η_1	α_1	$\phi_1''(0)$
0	3.51602	3.51602	0.48530	-0.91767	-2.17943
0.1	3.55870	3.55870	0.46527	-0.67839	-2.77629
0.2	3.60827	3.60828	0.44358	-0.46225	-3.81950
0.3	3.66675	3.66675	0.42008	-0.26964	-6.10547
0.4	3.73708	3.73708	0.39453	-0.10104	-15.0964
0.5	3.82378	3.82379	0.36666	0.04295	32.6565
0.6	3.93428	3.93428	0.33614	0.16152	7.90799
0.7	4.08177	4.08171	0.30258	0.25365	4.53260
0.8	4.29722	4.29249	0.26552	0.31791	3.20978
0.9	4.69688	4.63072	0.22496	0.35413	2.54541

6.4 Simulation Results and Discussion

In order to show the performance of control system for solving vibration and positioning problems, the responses of the beam rotational motion and the beam tip vibration to the step input are determined separately for different taper ratios. For the

uniform situation, the following parameter values are used: ζ_1=0.7, ζ_{s1_1}=0.7, ω_1=2 rad/s. For any other situation, these parameters are calculated by using Equation (6.48). The responses are found as in Figure 6.3.

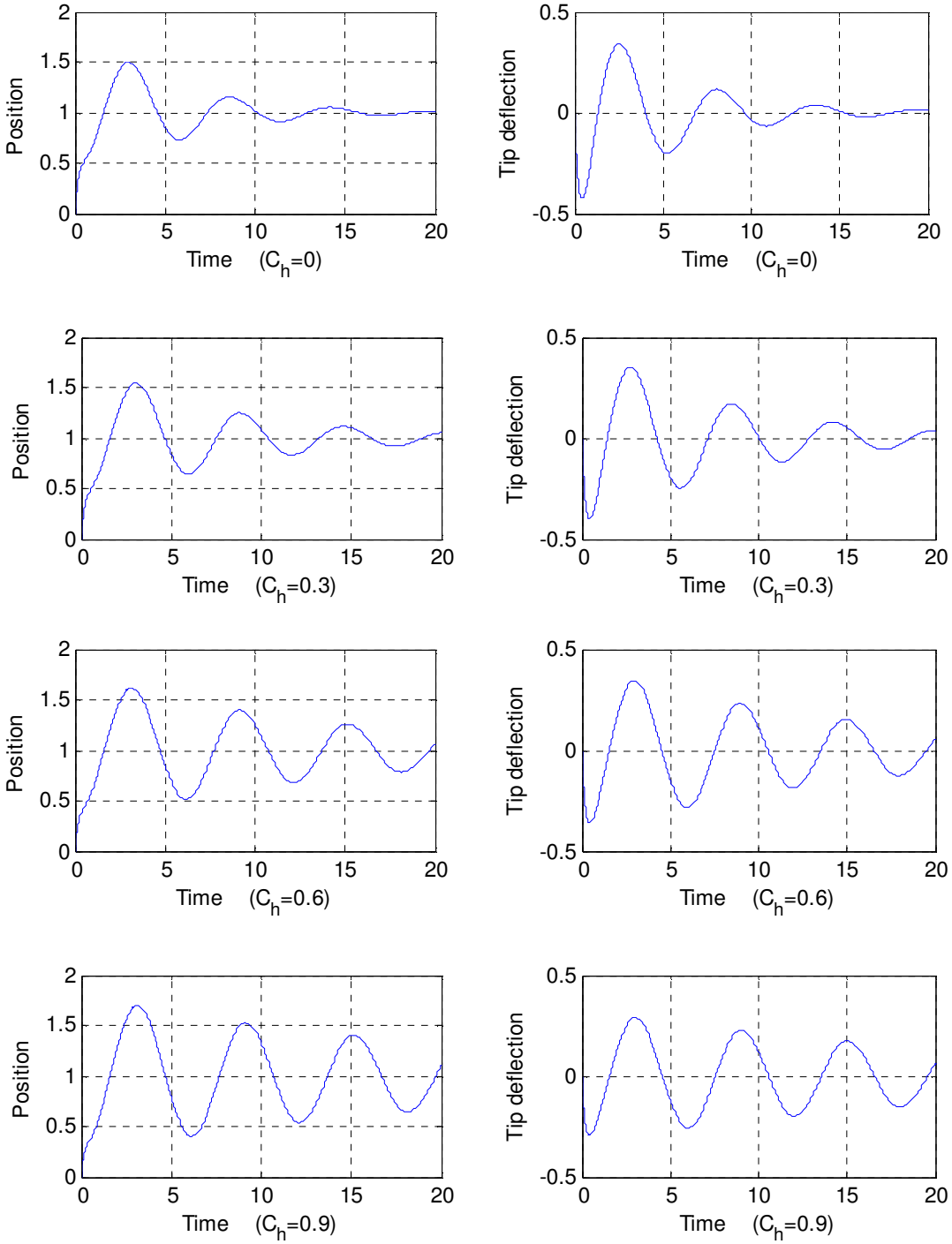


Figure 6.3 : Step responses for different taper ratios

In Table 6.2, effect of the taper ratio on the responses is given. Here it is seen that increasing the taper ratio makes maximum overshoot of beam rotational motion higher. On the other hand, maximum amplitude of beam tip motion becomes lower. In both situations, responses become more oscillatory.

Table 6.2: Effect of taper ratio on beam responses

c_h	Maximum overshoot of beam rotational motion	Maximum amplitude of beam tip motion
0	0.4973	0.4274
0.1	0.5108	0.4194
0.2	0.5264	0.4103
0.3	0.5445	0.3999
0.4	0.5653	0.3879
0.5	0.5890	0.3741
0.6	0.6160	0.3581
0.7	0.6459	0.3393
0.8	0.6772	0.3171
0.9	0.6972	0.2914

In Table 6.3, effect of the taper ratio on the system poles is considered. Here $s_2, s_3,$ and s_4 are inclined toward the imaginary axis and s_1 is inclined away from the imaginary axis while increasing the taper ratio. Also, the system tends to become less damped while increasing the taper ratio since the system poles mostly tend to come close to the imaginary axis.

Table 6.3 : Effect of taper ratio on the system poles

c_h	s_1	s_2	s_3, s_4
0	-3.8318	-1.2058	-0.2012 ± 1.1221i
0.1	-4.0412	-1.1084	-0.1765 ± 1.1140i
0.2	-4.2488	-1.0259	-0.1524 ± 1.1037i
0.3	-4.4626	-0.9544	-0.1294 ± 1.0913i
0.4	-4.6901	-0.8913	-0.1075 ± 1.0775i
0.5	-4.9402	-0.8351	-0.0871 ± 1.0626i
0.6	-5.2249	-0.7845	-0.0685 ± 1.0476i
0.7	-5.5604	-0.7391	-0.0522 ± 1.0340i
0.8	-5.9640	-0.6995	-0.0431 ± 1.0462i
0.9	-6.3836	-0.6735	-0.0401 ± 1.0262i

7. CONCLUSION

In this thesis, mainly vibration analysis and system control of rotating structures has been examined widely.

After a short introduction in the first chapter, in the second chapter control system has been defined and the steps used for modelling a control system have been introduced. In addition to this, some extra informations to develop controlling model used in this study have been given. In the thirh and fifth chapter derivation of equation of motion and free vibration analysis have been done. In the sixth chapter by using dynamic equations and structural parameters found with DTM, vibration control of rotating, tapered, clamped-free Euler-Bernoulli has been done. Also, the results are discussed in this chapter.

REFERENCES

Abdel, I.H. and Hassan, H., 2002: On solvig some eigenvalue-problems by using a differential tarnsformation, Appl. Math. Comput., 127, 1-22

Chiou, J.S. and Tzeng, J.R., 1996: Application of the Taylor transform to nonlinear vibration problems, J. Vib. Acoust., 118, 83-87

Diken H., 2000: Vibration control of a rotating Euler-Bernaulli beam, J. Sound Vibration, 232, 541-551

Fu K.S. and Gonzales R.C., 1987: Robotics: Control, sensing, vision and intelligence

Hodges D.H. and Pierce G.A., 2002: Introduction to structural dynamics and aeroelasticity, 1th Edition

Jang, M.J., Chen, C.L. and Liu, Y.C., 2001: Two-dimensional differential transform for partial differential equations, Appl Math Comput, 121, 261-270

Kuo C.B. and Golnaraghi, F., 2003: Automatic control systems, 8th Edition

Oktay T., Özdemir Ö. ve Kaya M.O., 2008: Dönen ve daralan Euler-Bernoulli kirişinin titreşim kontrolü, II. ULUSAL HAVACILIK VE UZAY KONFERANSI, UHUK-2008-076

Özdemir, Ö. and Kaya, M. O., 2006: Flexural vibration analysis of double tapered rotating Euler-Bernoulli beam by using the Differential Transform Method, Meccanica, 41, 661-670.

Wang F.Y. and Gao Y., 2003: Advanced studies of flexible robotic manipulators: Modeling, Design, Control and Applications, 4th Edition

Zhou, J.K., 1986: Differential transformation and its application for electrical curcuits, Huazhong University Press, P.R. China

Zhu W.D. and Mote C.D., 1997: Dynamic modeling and optimal control of rotating Euler-Bernaulli beams, J. Dynamic Systems, Measurement, and Control, 119, 802-808

APPENDIX

Sample Matlam-M code for beam rotational motion:

```
% % % % % % % % % %% % % % % % % % % % % % % % % % % % % % % % % % % % % % % % %
% % % %   VIBRATION CONTROL OF ROTATING EULER-BERNOULLI BEAM
% % % %   Beam Rotational Motion
% % % %   Tugrul Oktay, Istanbul Technical University
% % % % % % % % % %% % % % % % % % % % % % % % % % % % % % % % % % % % % % % % %
% Structural parameters for rotating Euler-Bernoulli beam
n=2;
alfa1=-0.917671; alfa2=-0.678391;  alfa3=-0.462252;  alfa4=-0.269642;
alfa5=-0.10104;   alfa6=0.0429457;  alfa7=0.161523;   alfa8=0.253648;
alfa9=0.31791;
fi1=-2.17943;      fi2=-2.77629;      fi3=-3.8195;       fi4=-6.10547;
fi5=-15.0964;      fi6=32.6565;       fi7=7.90799;       fi8=4.5326;
fi9=3.20978;
nu1=0.4853;        nu2=0.465269;      nu3=0.443581;      nu4=0.42008 ;
nu5=0.394532;      nu6=0.366659;      nu7=0.336136 ;     nu8=0.302576;
nu9=0.265552;
w1=3.51602;        w2=3.5587;         w3=3.60827;        w4=3.66675 ;
w5=3.73708;        w6=3.82378;        w7=3.93428 ;       w8=4.08177;
w9=4.29722;
% % % % % % % % % %% % % % % % % % % % % % % % % % % % % % % % % % % % % % % % %
% Taper ratios
c1=0;   c2=0.1;  c3=0.2;  c4=0.3;   c5=0.4;
c6=0.5; c7=0.6;  c8=0.7;  c9=0.8;
cb=0;
% % % % % % % % % %% % % % % % % % % % % % % % % % % % % % % % % % % % % % % % %
a1=((40-15*(c1+cb)+12*c1*cb)^0.5) /((40-15*(c1+cb)+12*c1*cb)^0.5);
a2=((40-15*(c1+cb)+12*c1*cb)^0.5) /((40-15*(c2+cb)+12*c2*cb)^0.5);
a3=((40-15*(c1+cb)+12*c1*cb)^0.5) /((40-15*(c3+cb)+12*c3*cb)^0.5);
a4=((40-15*(c1+cb)+12*c1*cb)^0.5) /((40-15*(c4+cb)+12*c4*cb)^0.5);
a5=((40-15*(c1+cb)+12*c1*cb)^0.5) /((40-15*(c5+cb)+12*c5*cb)^0.5);
a6=((40-15*(c1+cb)+12*c1*cb)^0.5) /((40-15*(c6+cb)+12*c6*cb)^0.5);
a7=((40-15*(c1+cb)+12*c1*cb)^0.5) /((40-15*(c7+cb)+12*c7*cb)^0.5);
a8=((40-15*(c1+cb)+12*c1*cb)^0.5) /((40-15*(c8+cb)+12*c8*cb)^0.5);
a9=((40-15*(c1+cb)+12*c1*cb)^0.5) /((40-15*(c9+cb)+12*c9*cb)^0.5);
% % % % % % % % % %% % % % % % % % % % % % % % % % % % % % % % % % % % % % % % %
ro1=w1/(n*a1); ro2=w2/(n*a2);  ro3=w3/(n*a3);  ro4=w4/(n*a4);
ro5=w5/(n*a5); ro6=w6/(n*a6);  ro7=w7/(n*a7);  ro8=w8/(n*a8);
ro9=w9/(n*a9);
% % % % % % % % % %% % % % % % % % % % % % % % % % % % % % % % % % % % % % % % %
```

```
zetas1=0.7*((alfa1*fi1)/ ((-0.917671)*(-2.17943))) *a1;
zetas2=0.7*((alfa2*fi2)/ ((-0.917671)*(-2.17943))) *a2;
zetas3=0.7*((alfa3*fi3)/ ((-0.917671)*(-2.17943)))* a3;
zetas4=0.7*((alfa4*fi4) /((-0.917671)*(-2.17943))) *a4;
zetas5=0.7* ((alfa5*fi5) /((-0.917671)*(-2.17943))) *a5;
zetas6=0.7*((alfa6*fi6)/((-0.917671)*(-2.17943))) *a6;
zetas7=0.7*((alfa7*fi7) /((-0.917671)*(-2.17943))) *a7;
zetas8=0.7*((alfa8*fi8) /((-0.917671)*(-2.17943))) *a8;
zetas9=0.7*((alfa9*fi9) /((-0.917671)*(-2.17943))) *a9;
% % % % % % % % % %% % % % % % % % % % % % % % % % % % % % % % % % %
zeta1=0.7*a1; zeta2=0.7*a2; zeta3=0.7*a3; zeta4=0.7*a4;
zeta5=0.7*a5; zeta6=0.7*a6; zeta7=0.7*a7; zeta8=0.7*a8;
zeta9=0.7*a9;
% % % % % % % % % %% % % % % % % % % % % % % % % % % % % % % % % % %
gama1=(zeta1/zetas1); gama2=(zeta2/zetas2); gama3=(zeta3/zetas3);
gama4=(zeta4/zetas4); gama5=(zeta5/zetas5); gama6=(zeta6/zetas6);
gama7=(zeta7/zetas7); gama8=(zeta8/zetas8); gama9=(zeta9/zetas9);
% % % % % % % % % %% % % % % % % % % % % % % % % % % % % % % % % % %
n1=[ 2*zeta1  1  2*zeta1*ro1^2  ro1^2]; n2=[ 2*zeta2  1  2*zeta2*ro2^2  ro2^2];
n3=[ 2*zeta3  1  2*zeta3*ro3^2  ro3^2]; n4=[ 2*zeta4  1  2*zeta4*ro4^2  ro4^2];
n5=[ 2*zeta5  1  2*zeta5*ro5^2  ro5^2]; n6=[ 2*zeta6  1  2*zeta6*ro6^2  ro6^2];
n7=[ 2*zeta7  1  2*zeta7*ro7^2  ro7^2]; n8=[ 2*zeta8  1  2*zeta8*ro8^2  ro8^2];
n9=[ 2*zeta9  1  2*zeta9*ro9^2  ro9^2];
% % % % % % % % % %% % % % % % % % % % % % % % % % % % % % % % % % %
d1=[(1-nu1)  2*zeta1*(1+gama1)  (ro1^2+1)  (2*zeta1*ro1^2)  ro1^2 ];
d2=[(1-nu2)  2*zeta2*(1+gama2)  (ro2^2+1)  (2*zeta2*ro2^2)  ro2^2 ];
d3=[(1-nu3)  2*zeta3*(1+gama3)  (ro3^2+1)  (2*zeta3*ro3^2)  ro3^2 ];
d4=[(1-nu4)  2*zeta4*(1+gama4)  (ro4^2+1)  (2*zeta4*ro4^2)  ro4^2 ];
d5=[(1-nu5)  2*zeta5*(1+gama5)  (ro5^2+1)  (2*zeta5*ro5^2)  ro5^2 ];
d6=[(1-nu6)  2*zeta6*(1+gama6)  (ro6^2+1)  (2*zeta6*ro6^2)  ro6^2 ];
d7=[(1-nu7)  2*zeta7*(1+gama7)  (ro7^2+1)  (2*zeta7*ro7^2)  ro7^2 ];
d8=[(1-nu8)  2*zeta8*(1+gama8)  (ro8^2+1)  (2*zeta8*ro8^2)  ro8^2 ];
d9=[(1-nu9)  2*zeta9*(1+gama9)  (ro9^2+1)  (2*zeta9*ro9^2)  ro9^2 ];
% % % % % % % % % %% % % % % % % % % % % % % % % % % % % % % % % % %
t=0:0.002:20;
[y1,x,t]=step(n1,d1,t); [y2,x,t]=step(n2,d2,t);
[y3,x,t]=step(n3,d3,t);
[y4,x,t]=step(n4,d4,t); [y5,x,t]=step(n5,d5,t);
[y6,x,t]=step(n6,d6,t);
[y7,x,t]=step(n7,d7,t); [y8,x,t]=step(n8,d8,t);
[y9,x,t]=step(n9,d9,t;
plot(t,y1,t,y2,t,y3,t,y4,t,y5,t,y6,t,y7,t,y8,t,y9)
grid
xlabel ('Time    (c_h=0, c_b=0)') ; ylabel('Position');
axis([0 20 0 2])
% % % % % % % % % %% % % % % % % % % % % % % % % % % % % % % % % % %
```

CURRICULUM VITAE

I was born in Ordu in 1984. I graduated from Ordu High School in 2002 and at the same year I came to ITU. I studied in Aeronautical Engineering Department for four years. I graduated from Aeronautical Engineering in June 2007. I am still continuing my studies as M.S. student in Istanbul Technical University, Aeronatical and Astronautical Engineering Department.